Heliyon 8 (2022) e09779

Contents lists available at ScienceDirect

Heliyon

journal homepage: www.cell.com/heliyon

Research article

Potential effects of Land Use Land Cover Change on streamflow over the Sokoto Rima River Basin

Ifeanyi Chukwudi Achugbu[a,b,c,*], Ayo Akinlabi Olufayo[b], Ifeoluwa Adebowale Balogun[b], Jimy Dudhia[c], Molly McAllister[c], Elijah Adesanya Adefisan[b], Edward Naabil[d]

[a] Department of Water Resources Management and Agrometeorology, Federal University Oye-Ekiti, P. M. B. 373, Oye-Ekiti, Ekiti State, Nigeria
[b] West African Science Service Center on Climate Change and Adapted Land-Use (WASCAL), Federal University of Technology Akure, Akure, Ondo State, Nigeria
[c] National Center for Atmospheric Research, P. O. Box 3000, Boulder, Colorado, USA
[d] Department of Agricultural Engineering, Bolgatanga Technical University, P O Box 767, Bolgatanga, Ghana

ARTICLE INFO

Keywords:
Weather research and forecasting (WRF) hydrological model
Land use land cover change (LULCC)
Streamflow
Savanna
Grassland

ABSTRACT

This research investigated the effects of Land Use Land Cover Change (LULCC) over the Sokoto Rima River Basin (SRRB) using a setup of Weather Research and Forecasting (WRF) atmospheric model to generate the parameters to force WRF hydrological (WRF-Hydro) model which comprises of a parent domain at 12km horizontal resolution with an updated MODIS Land Use (LU) data and the nested domain at 4km resolution which focuses on the SRRB. The calibration of the model was done by modifying the infiltration and the Manning's roughness parameters. WRF-Hydro model was used to run simulations with the control LU and five different LU scenarios generated for Urban (Ur), Grassland (Gr), Savanna (Sa), Forest (Fr) and Barren (Ba). For the period analysed, simulation with Gr scenario increased streamflow in all the forecast points, while the Sa decreases it. A strong correlation was noted between the input precipitation and streamflow for all LU scenarios, and a significant Specific Discharge to Rainfall (SDR) for Ur, Fr and Ba scenarios. There was an increase in streamflow in the dry period due to afforestation and a decrease due to deforestation. Areas where grasslands were converted into savanna showed a little increase in evapotranspiration ET. There was more ET for the Sa scenario than the Gr scenario in the wet period, while there was more ET in the dry period for Gr scenario than it is for the Sa scenario. The study has shown that ET is a major factor to changes in streamflow due to LU changes over the basin. The sensitivity of the model to LULCC is reasonable, but more research is recommended to compare results with different hydrological model popularly used for LULCC impact studies.

1. Introduction

Land Use Land Cover Change (LULCC) is a vital attribute in the runoff procedure, which has an effect on erosion, interception, infiltration and evapotranspiration (Alemayehu, 2015). Land Use (LU) change could interrupt the hydrological cycle by means of increasing the water yield, causing a reduction or at times completely removing the low flow (Pereira 1989; Croke et al., 2004). The decrease in water recycling and evapotranspiration as a result of changes in Land Use Land Cover (LULC) could trigger a feedback mechanism in which the consequence is reduced rainfall (Savenije 1995). Alterations in the attributes of land surface influences the surface water balance (Pitman, 2003).

Regarding the hydrologic implication of LULCC, according to Shuster et al. (2005) and Zhou and Wang (2008), Impervious Surface Area (ISA) of an urban settlement is often used to study the environmental impact of urbanization. The expansion of the ISA affects a series of hydrologic processes as it reduces infiltration and baseflow, increases peak flow and runoff, and raises the accumulation of sediment (Zhou 2014) and thereby leading to some environmental problems namely flooding, erosion, sedimentation, higher air temperatures, alteration in the habitat, and reduction in the population of fishes.

LULCC and its related consequences are recognised to influence the hydrology of the basin (Foley et al., 2005; Ohana-Levi et al., 2015; Kumar et al., 2018, Patil and Nataraja 2020; Thiha et al., 2020; Khoi et al., 2021 e.t.c.). Researchers like Lal (1997) and Ngana (2002) have stated that the impact of vegetation cover in improving the capacity of basins, moisture conservation and water yield increase cannot be disregarded. This is because it can alter the hydrological flow regime of the river catchments.

* Corresponding author.
E-mail address: ifeanyi.chukwudi@fuoye.edu.ng (I.C. Achugbu).

https://doi.org/10.1016/j.heliyon.2022.e09779
Received 4 January 2022; Received in revised form 28 April 2022; Accepted 20 June 2022

Exchange of heat in the space separating land and the atmosphere could be affected by loss of wetlands, which can considerably adjust evapotranspiration and runoff (Bartzen et al., 2010). Also, the changing of wetlands to agricultural lands can likewise lead to alterations in composition and role of vegetation layer that further affects the energy fluxes in climate system (Carrington et al., 2001). Furthermore, the transformation of wetlands to urban construction areas enlarges the watertight surfaces like houses, parking grounds, and highways which permits no infiltration, hence will turn all the water that drops on them into run-off, and thus influence regional water cycling (Li et al., 2018). According to Zheng et al. (2008), changes in land use types in a catchment could have a considerable effect on the streamflow/discharge and its response to storms.

Using various modeling techniques over West Africa, researchers such as Aduah et al. (2017); Li et al. (2007) and Akpoti et al. (2016) have all emphasized that deforestation results into an increase in runoff over West Africa using Agricultural Catchments Research Unit (ACRU) model, SWAT model and Integrated Biosphere Simulator (IBIS) respectively. Li et al. (2007) also affirmed that when land cover change exceeds some thresholds, the water yield was increased substantially. Zhou (2014) emphasized that although much progress has been made in the study of hydrologic impact of LULCC, there are still numerous uncertainties and even controversies. There are uncertainties from data sources, LULCC quantification, and hydrologic modeling in the evaluation. The hydrologic impact of LULCC may vary with study area, climate condition, geography, and spatial scale, and it is also dependent on the temporal scale analyzed. All of these factors make the evaluation of the hydrologic impact of LULCC more challenging and never-ending.

The study area, Sokoto Rima River Basin (SRRB), is extremely suceptible to the alterations that affects hydrological processes, which have led to the reduction of water in the available reservoirs. Because of the semi-arid nature of most parts of the catchment, it suffered heavily during the 1970's and the 80's Sahelian drought. The catchment is also being confronted with high erosion due to high rainfall between July and September each year, which also worsens the LULCC of the catchment. Unceasing LULCC has the potential to affect the water balance of a catchment by altering the size and order of the constituents of streamflow. However, the study of LULCC impacts on streamflow has been one area that is sparsely carried out in West Africa. This could be because of the sparseness of hydrometeorological data of good standard over the region (Jones et al., 2015). So, as the practice of agriculture also entails deforestation, the question is how would change in land cover affect the flow over the basin that is already faced with perpetual drought? Another important question is that what will be the future situation if deforestation is not checked, and if afforestation is greatly practiced? The existence of a basin especially in a Sudano-Sahelian environment is sure to increase livelihood, assure food security, reduce hunger, improve production and provide job for the people around and beyond. Nevertheless, the evaluation of the prevailing and possible LULCC on streamflow in the basin is quite compulsory for LU design. This is an essential condition for a viable water resources management, hence the need for this research over the basin.

The aim of this research is to simulate the response of streamflow to alterations in LULCC scenarios in the SRRB. Many researchers have worked on the effects of LULCC on different river catchment areas in the Niger basin and in West Africa within and outside Nigeria using different tools and approaches like remote sensing, statistical and modeling tools, but none have either used the WRF-Hydro model, or incorporated a satellite data into the model. In regards to calibration, processes involved, usage and complexity, models could be different from each other. Actually, there is no one-size-fits-all model for all applications (Merritt et al., 2003). Hence, the choice of a specific model is aimed at getting adequate solution to a particular problem. However, this research uses the WRF and WRF-Hydro model to simulate the impact of LULCC on streamflow over the SRRB in West Africa.

2. Data and methodology

2.1. Study area

The SRRB is a semi-arid basin, which lies in the Sudano-Sahelian zone of West Africa with mostly Savanna vegetation and marked with a

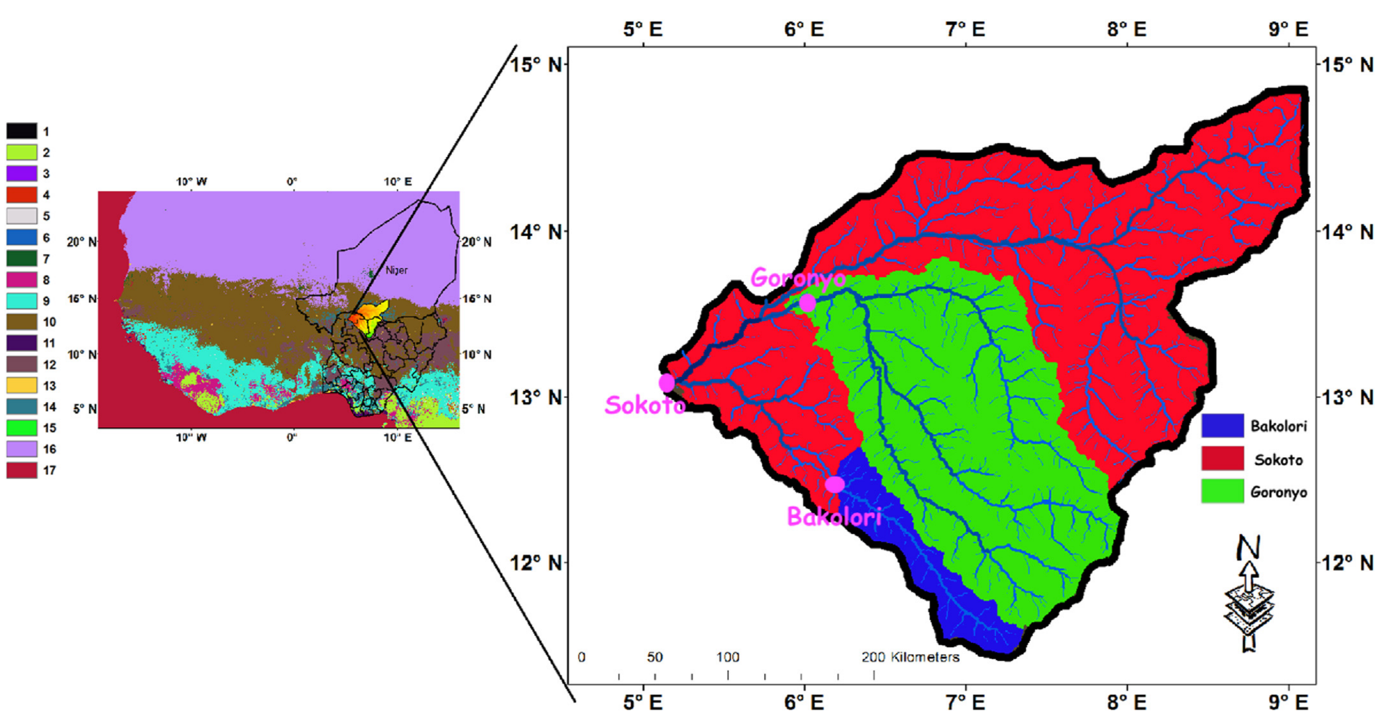

Figure 1. Position of SRRB in West Africa, also showing the Streamflow Order, the basin mask and the location of the three Forecast Points (the purple-coloured points). The legend parameters value is same as in Appendix 1.

separate dry and wet season. The complete SRRB lies between latitudes 10°**N** and 16°N with northern extension to Niger and longitudes 3°E and 9°E and covering an area over 100,000 square kilometres and bodering with Benin Republic on the southwest. The SRRB covers Zamfara, Sokoto, Kebbi and Katsina states in Nigeria to the East, and is bounded to the Southeast by Niger State in Nigeria. Two major dams, which include the Goronyo and Bakolori dams, were situated in the basin mainly for water supply, irrigation and other agricultural purposes. However, there are about 12 other Dams and tangible diversions located within the basin. These have the tendency to reduce the flow downstream as Armitage and Petts (1992) stressed that river abstraction reduces the volume of discharge that as a response could change the width, depth, velocity pattern and shear stresses within the river channel.

According to Ekpoh and Ekpeyong (2011), average annual temperature for Sokoto is 34.5°C, even though dry season temperatures may exceed 40°C in some years around February and April within the region. The daily minimum temperature may be lower than 18°C during the harmattan season. According to Abdullahi et al., (2014), the basin is characterized with high evaporation, which could be about 80mm in July and around 210mm in April to May. April to May is the period with highest evaporation and also the hottest months. In April, Relative Humidity (RH) is close to 19%, and gets to about 64% in August. Rainfall in the basin is seasonal. Sokoto has an average annual rainfall of 629mm (Ekoh 2020). The rainy season usually commences from May or June and could last till September or early October based on the yearly rainfall pattern, so nearly all the rain falls within May and September. Also, the northern part is dominantly shrubby and thorny vegetation known for the Sahel region of West Africa. The area under study is a sub basin in the SRRB which is situated amid 11°30′N and 15°N and 5°E and 9°10′E (Figure 1), covering an area of about 65,000 square kilometres. It covers Sokoto, Zamfara, Katsina, small part of Jigawa and Kano. The reason for selecting a smaller domain was due to the high computational cost of running WRF-Hydro simulations over such a very huge domain. In addition, building the routing grids using the WRF-Hydro Geographic Information System (GIS) pre-processing tools was also difficult for a larger domain. The basin masks show the area drained to each Forecast Point (FP), which includes Sokoto, Goronyo and Bakolori. Both Goronyo and Bakolori drained into the Sokot FP.

The dominant LU parameters in the basin (based on the 2012 LU data obtained from MCD12Q1 data) includes Grasslands occupying about 22.18% of the area, Croplands occupying about 50.12% of the area, Urban and built-up lands occupying about 0.63% of the area, Cropland/Natural vegetation Mosaics occupying about 26.54% of the area and Barren lands covers 0.51% of the area.

2.2. Data

2.2.1. Observed data

The all-important in-situ streamflow data available is located at the Goronyo dam, which is the in-flow to the dam. The data is available since the inception of the dam, but due to inconsistency and loss of records, only 2012 to 2013 were made available. Although, promises were made by the dam management to release more recent streamflow data in the future, but we have to make use of what was made available.

2.2.2. Land Use Land Cover data

The default LU in WRF model is the Moderate Resolution Imaging Spectroradiometer (MODIS) data, which is based on the 2001 data archive, and is yet to be updated for West Africa. This research therefore integrated an updated collection 6 (C6) MODIS Land Cover Type Product (MCD12Q1) into the model. The MCD12Q1 made available a yearly global LU map of 500m spatial resolution from 2001 until the present date. The land cover classification based on the International Geosphere-Biosphere Programme (IGBP) (Loveland and Belward 1997; Belward et al., 1999) of MCD12Q1 MODIS land use data was selected for the research.

The accuracy assessment of the MCD12Q1 data revealed that C6 product has an all-inclusive accuracy of 73.6%. Also, the number of bogus LC change has been considerably reduced in C6 in comparison with C5 (16% in C6 and 11.4% in C5) (Sulla-Menashe et al., 2019). Reason for the choice of IGBP land cover classification in this research is because of its near match with the default LU data in WRF. The name of

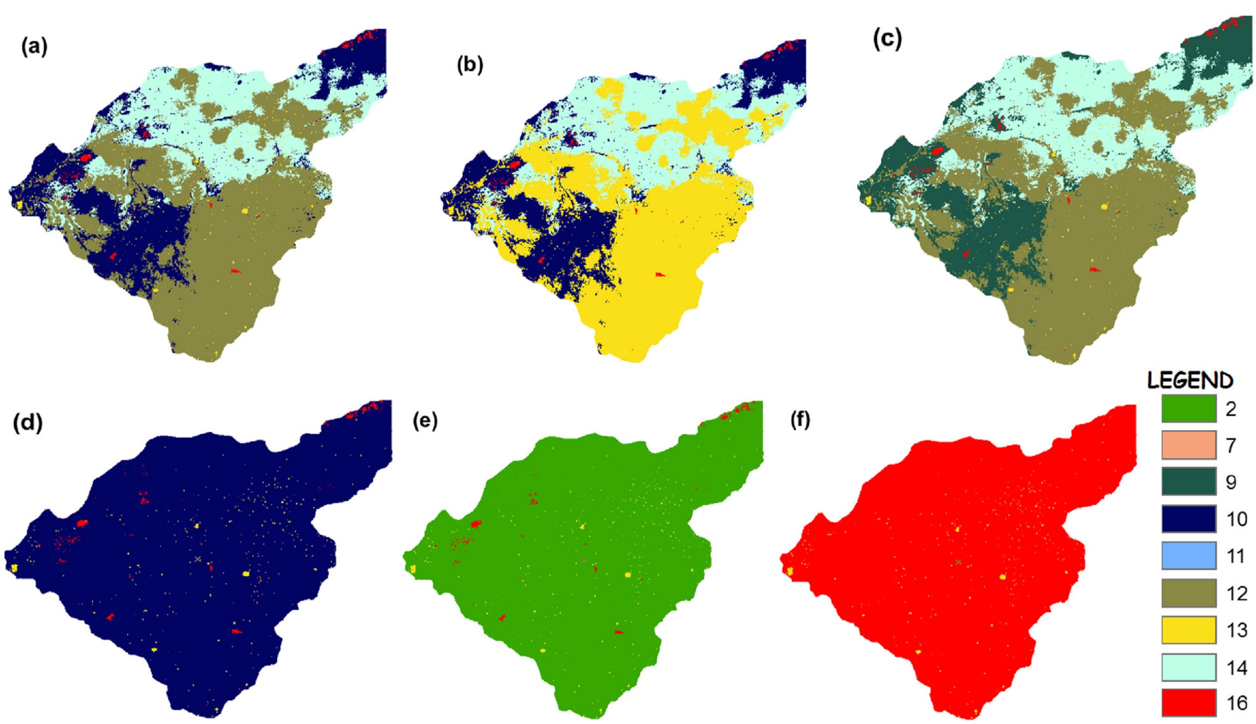

Figure 2. Various LULCC scenarios utilized for the Simulations over the SRRB (a) 2012 control, (b) Urban, (c) Savanna (d) Grassland (e) Forest (f) Barren. Legend Parameters: Evergreen broadleaf forests 2, Open shrublands 7, Savannas 9, Grasslands 10, Permanent wetlands 11, Croplands 12, Urban and built-up lands 13, Cropland/Natural vegetation mosaics 14, and Barren 16.

Table 1. The percentage coverage of each LU variable with regards to the pixel counts for each scenario over SRRB.

LU Parameters	Code	Ct	Ur	Sa	Gr	Fr	Ba
Evergreen Broadleaf Forests	2	0.000	0.000	0.000	0.000	98.859	0.000
Open Shrublands	7	0.011	0.011	0.011	0.000	0.000	0.000
Savannas	9	0.000	0.000	22.180	0.011	0.000	0.000
Grasslands	10	22.180	22.180	0.000	98.849	0.000	0.000
Wetlands	11	0.001	0.000	0.001	0.001	0.001	0.001
Croplands	12	50.126	0.000	50.126	0.000	0.000	0.000
Urban Lands	13	0.630	50.757	0.630	0.630	0.630	0.630
Cropland/Natural Vegetation Mosaics	14	26.543	26.543	26.543	0.000	0.000	0.000
Barren	16	0.510	0.510	0.510	0.510	0.510	99.369

*Ct, Ur, Sa, Gr, Fr and Ba are the LULCC scenarios for SRRB, i.e., Control, Urban, Savanna, Grassland, Forest and Barren, respectively.

the IGBP LU parameter, the assigned value of the name, and the description of the components, which the parameter names are made up of, are presented in Appendix 1. Some of the parameters in some instance could not fill up the size of the pixel due to its lower resolution, and hence were mixed with other parameters.

2.2.3. Generation of the LULCC scenarios

The granule of MODIS MCD12Q1 data that covers the basin was downloaded from the MODIS website https://searchearthdatanasagov/. The data are in sinusoidal projection, hence was, resampled and reprojected to WRF projection. In order to study the response of streamflow to different land cover scenarios in the Sokoto Rima River Basin (SRRB), five various LC scenarios were created; Urban (Ur), Grassland (Gr), Savanna (Sa), Forest (Fr) and Barren (Ba) as shown in Figure 2. The LULCC scenarios were developed by changing some LU parameters into another as follows: for Ur scenario, all croplands were converted into Urban and Built-up Lands; for Sa, Grasslands was changed into Savannas; for Gr, croplands and Cropland/Natural Vegetation Mosaics were converted into Grasslands, after that, Open shrublands was converted into Savannas; for Fr, Open Shrublands, Grasslands, Croplands and Cropland/Natural Vegetation Mosaics were all converted into evergreen broadleaf forests; for Ba, open shrublands, Grasslands, Croplands and Cropland/Natural Vegetation Mosaics were all converted to Barren lands.

The Gr scenario was conceived in that most a time during the dry season, part of the area is usually razed by fire, which at times could be deliberate in order to have a fresh growth of grasses when rain comes. As Savanna is grassland with scattered individual trees, the Sa was conceived in order to see how the inclusion/planting of trees to grasslands could impact the streamflow over the basin. In the studies from LULCC impacts, uncertainties resulting from observed data, the parameterization process, and the conceptual model cannot be rulled out (Aboelnour et al., 2020). Hence, to be sure and clearly recognize the effect of urbanization, afforestation and deforestation on the basin, and that the effects can be truly and distinctly simulated, this necessitates the hypothesizing of extreme LULCC that could be legibly sensitive to the changes from the model other than a naturally or feasibly occurring condition. Hence, the reason for the inclusion of some perhaps unrealistic extreme LULCC scenarios (i.e., the Ur, Fr and Ba) as it also gives room to study and have a comprehensible explanation of the processes through which LULCC affects streamflow. However, our discussion is mostly based on the Sa and Gr scenarios.

Table 1 presents the percentage coverage of each LU variable with regards to the pixel counts for the Control (Ct) and each land use Scenario over the basin. Version 5.0 of the WRF-Hydro modelling system (Gochis et al., 2018) forced with WRFV3.9.1.1 outputs was employed to simulate the response of streamflow to different land cover scenarios over the Sokoto Rima River Basin (SRRB).

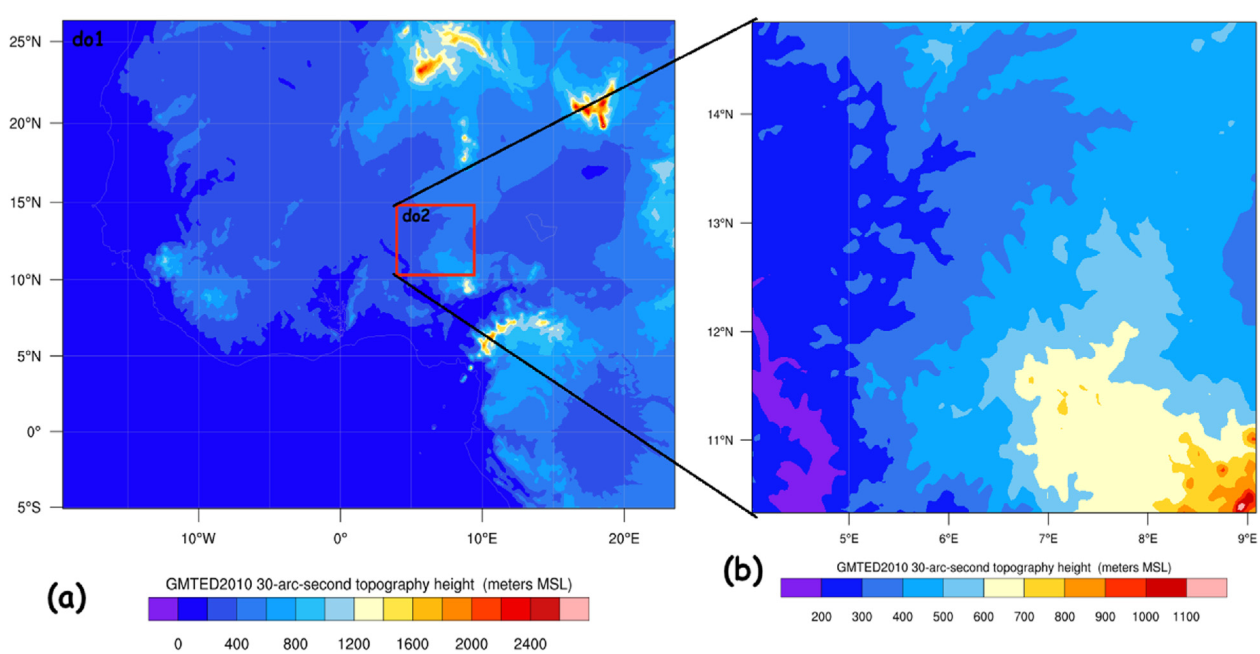

Figure 3. Terrain of WRF domain for the WRF-Hydro Simulations; (a) do1 is the main domain at 12 km and do2 is the nested domain for WRF-Hydro Simulations, and (b) the nested domain at high resolution of 4 km.

Table 2. WRF physics parameterisations used.

Physics Schemes	Selected parameterisation options	Reference
Cumulus Parameterisation	New Tiedtke scheme	Zhang et al. (2011)
Longwave Radiation	New version of Rappid Radiative Transfer Model (RRTMG)	Iacono et al. (2008)
Microphysics	WRF Single-Moment 6-class (WSM6)	Hong and Lim (2006)
Planetary Boundary layer	Mellow-Yamada Nakanishi and Niino Level 25 (MYNN25)	Nakanishi and Niino (2006)
Shortwave Radiation	New version of Rappid Radiative Transfer Model (RRTMG)	Iacono et al. (2008)
Land Surface	Noah-Multi Physics (Noah-MP)	Niu et al. (2011)

2.3. Atmospheric and hydrological modelling system

2.3.1. WRF atmospheric model and WRF-hydrological model (WRF-hydro)

WRF atmospheric model has been extensively used among researchers and is suitable for use in diverse scales, ranging from one or two to thousands of kilometers. WRF hydrological model (WRF-Hydro) was developed to improve the delineation of the hydrological processes over land. Version 5.0 was used in this research. Kannan et al. (2019) identified some of the challenges to large-scale hydrologic model calibration which includes the accessibility of reliable quality data, consideration of several reservoirs present in a sub-basin, poor representation of elevation and slopes in highland areas, description of the carrying capacity of river channels, exclusion of some section of the basin because of administrative boundary problems, poor replication of irrigation return flows, insufficient description of vegetation cover and soil types, poor representation of groundwater and surface abstractions, and inadequate representation of water releases between rivers. The baseflow into the stream network in the model is described with the use of a bucket model (Naabil et al., 2017). However, due to a high level of river abstractions and diversions through several dams upstream of the forecast points in this study, the observed streamflow data was drastically reduced and far lower than the simulation. Nevertheless, in order to get the model calibrated, the bucket model was switched off owing to insuficient knowledge of the channel attributes, as the model could not account for the high abstraction and diversions going on in the basin. However, for the LULCC experiments, the baseflow was switched on in order to avoid any form of uncertainties that could arise from that.

2.3.2. Set up of WRF and WRF-hydro model

The setup of the atmospheric model (WRF) to generate the parameters to force the hydrological model (WRF-Hydro) as shown in Figure 3, comprises of a parent domain (Figure 3a) configured at a horizontal resolutoin of 12 km and the nested domain (Figure 3b) at 4 km. The boundary conditions were taken from the 6 hourly ERA-Interim reanalysis data, with 0.75° resolution (Dee et al., 2011) and the initial soil data i.e., sea surface temperature, soil moisture and temperature, were taken from the National Centers for Environmental Protection (NCEP) Final Analysis (FNL) 6 hourly data. Hence, the boundary conditions were being updated 6 hourly.

Since we were able to have the observed data for only 2012 and 2013, the model was calibrated for 2012, after which the model was ran for 2011–2013, using the whole of 2011 as the spin-up time to allow the model adapt to the sensitivity of catchment conditions. However, due to inadequate observation data and computational cost of running WRF and WRF-Hydro models, we had to limit our studies within the time scale (2012–2013) for the assessment of the impact of LULCC on streamflows over the geographical area. Validation was done for 2013, and same year was analysed. Noah-MP LSM was used with other physics combination based on some preparatory tests, which is also in agreement with the results of Gbode et al. (2018) as shown in Table 2.

Researchers like Sertel et al. (2011), Wen et al. (2012) and Case et al. (2012) have changed the land use data in WRF by intergrating satellite data for a more updated LU data to enhance the models outputs as aslo carried out in this study. The default land use data in WRF model was substituted with the 2012 MODIS land use data which is updated and more realistic in order to have a comparable control simulation with the experiments, and an improved WRF model output for the hydrological simulations.

Considering the fact that the horizontal resolution of the nested domain is 4 km, which falls within the convective permitting scale, in which the cumulus activities would be resolved, cumulus scheme was therefore switched off for the nested domain.

2.3.3. WRF-hydro model calibration

The model calibration and validation was carried out based on the discharge at Goronyo FP out of the three FPs. According to Naabil et al. (2017), calibration information from a separate basin of indistinguishable geographical features could be used as a basis in the calibration process. This however justifies the use of the model for other FPs based on the calibration for Goronyo FP in this study.

There are two important steps usually taken into consideration in the calibration processes. Firstly, the REFKDT parameter which is the parameter for infiltration partitioning, the RETDEPRTFAC i.e., the surface retention depth, and the SLOPE that governs deep drainage. Secondly, the roughness parameter (Manning's roughness, MannN) that controls the shape of the hydrograph. However, there were factors like insufficient data on channel geometric along with measured data that limits the automatic calibration of these parameters, which necessitate the use of manual calibration.

Hence, the model calibration was centered on the channel's infiltration factor (REFKDT) and MannN coefficient. The REFKDT is a tunable parameter that considerably controls the surface infiltration, and consequently the partitioning of runoff (Ma et al., 2021). Increasing the value of REFKDT decreases the surface run off and vice versa. So, the default values of the other parameters that were not calibrated were used as a result of the limitations earlier mentioned. Although, depending on the experience of the researchers, the manual method of calibration could give a more appropriate result (Yin et al., 2020). As the REFKDT and MannN parameters are predefined tabulated values and are consequently symbolised as global values for the entire model domain, this method makes it feasible to modify the model to match with the amount and rhythm of the observed flow (Yucel et al., 2015). Tested values of REFKDT during calibration were 3, 1.5, 1.0, 0.7, 0.6, and 0.5.

2.3.4. Assessment of WRF-hydro calibration

The optimum streamflow estimates during calibration were assessed using statistical measures e.g., Percentage Bias (PBias), Pearson's correlation coefficient (r) and Nash-Sutcliffe efficiency index (NSE). The equations for computing the listed statistical approaches are described below;

$$\mathrm{PBIAS} = \sum_{t=1}^{N} (q_t^{\,y} - q_t^{\,x}) \Big/ \sum_{t=1}^{N} q_t^{\,x} \ \mathrm{X}\ 100 \tag{1}$$

$$\mathrm{NSE} = 1 - \sum_{t=1}^{N} (q_t^{\,y} - q_t^{\,x})^2 \Big/ \sum_{t=1}^{N} (q_t^{\,x} - q^{mean})^2 \tag{2}$$

$$r = \frac{n(\sum xy) - (\sum x)(\sum y)}{\sqrt{n\sum x^2 - (\sum x)^2 n \sum y^2 - (\sum y)^2}} \tag{3}$$

where q is the streamflow, x is the observed, and y is the model value.

Table 3. Model performance with different parameters for Goronyo FP.

	REFKDT 3.0 (Def.)	REFKDT 1.5	REFKDT 1.0	REFKDT 0.7	REFKDT 0.6	REFKDT 0.5
Pearson Correlation (r)	0.87	0.54	0.90	**0.90**	0.91	0.91
Nash-Sutcliffe (NSE)	0.35	0.13	0.78	**0.78**	0.74	0.60
P-bias	-64.40	-60.48	-14.34	**-7.42**	31.98	53.39

The PBIAS measures the average propensity of the simulated value to either be larger or smaller than the observed value. Positive values show that the model bias is toward overestimation, whereas negative values are an indication of underestimation (Gupta et al., 2009). The NSE gives the relative size of the residual variance (called "noise") to the variance of the flows ("information") (Nash and Sutcliffe 1970). The value of NSE ranges from negative infinity to 1.0. Values that fall between 0.0 and 1.0 are taken as satisfactory. The Pearson's Correlation (r) measures the similarity in the spatial or temporal patterns between two datasets. Also, the ratios of Specific Discharge to Rainfall (SDR) as in Eq. (4) were calculated.

$$SDR = \frac{\text{Specific discharge}}{\text{Rainfall}} \tag{4}$$

As shown by Burbank et al. (2012) and Guzha et al. (2018), a high SDR is an indication that a high fraction of rainfall in the basin is converted into stream discharge while a smaller amount is retained in the soil profile, and vice verca.

3. Results and discussion

3.1. Model calibration and validation

Based on different REFKDT values, the performance of the streamflow calibration is summarized in Table 3. Simulations with REFKDT 1.0, 0.7, 0.6 and 0.5 all gave a good estimate compared to the observed flow as shown in Figure 4, but in other to have the best, all the statistics were considered for the best selection. The REFKDT 0.5 has a good correlation but with a high bias and low NSE value which made the other three (i.e., REFKDT 1.0, 0.7 and 0.6) to be more preferable. Among the best three calibration parameters, the REFKDT 0.7 was chosen for the WRF-Hydro simulations because of its low bias as compared to others as all the best three has good correlation and good NSE value. From Figure 5, the calibrated model satisfactorily captured the maximum peak streamflow with regards to the observed monthly streamflow at the Goronyo station.

Figure 6 shows the temporal variations in streamflow and precipitation for the entire basin. The plot clearly indicates the seasonal rainfall patterns (high during the JAS period, low or none during the DJF period), and the streamflow consequently follows the same pattern. However, the onset of the precipitation does not result in runoff owing to infiltration and channel characteristics, which can be viewed from the streamflow peak that transpired about three weeks after the peak rainfall. This shows about three weeks lag period amidst the hyetograph and the hydrograph.

3.2. Analysis of the effects of LULCC scenarios

In order to study the impact of LULCC on streamflow, WRF-Hydro was run with five different LULCC scenarios and result of the differences between the outputs from each scenario and the control run was analysed. The model (WRF-Hydro) have not been practically applied for LULCC impact studies on hydrological parameters, hence it is necessary to examine its applicability with a scenario that could bring very obvious changes to have a clearer description of the processes by which land use change could affect streamflow over the basin. This and other aforementioned reasons necessitated the generation of the Ur, Fr and the Ba scenarios. The conversion of all Permanent Wetlands (Pw) and Croplands (Cr) into Builtup lands (Ub) increased the streamflow by 59.21% in Sokoto, 104.15% in Goronyo and 117.08% in Bakolori. The complete conversion of all the Land Cover Parameters (LCPs) (excluding barren, Built-up lands and permanent wetlands) into Evergreen Broadleaf Forests (i.e., Fr scenario) decreased the streamflow by 31.47% in Sokoto, 35.12%

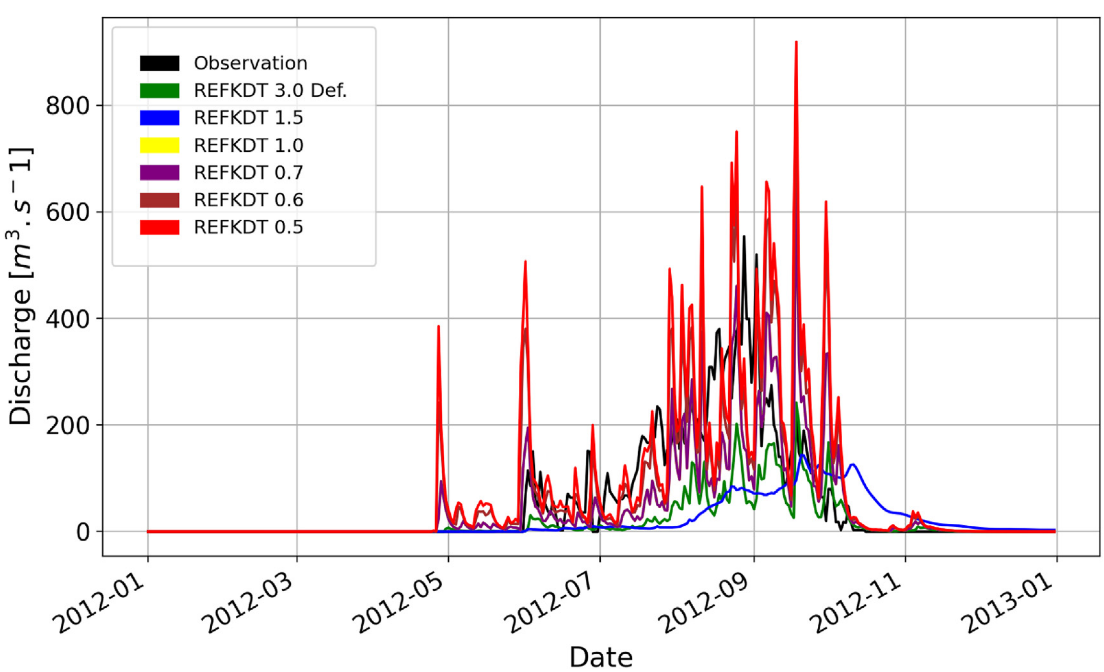

Figure 4. Streamflow calibration test for Goronyo FP.

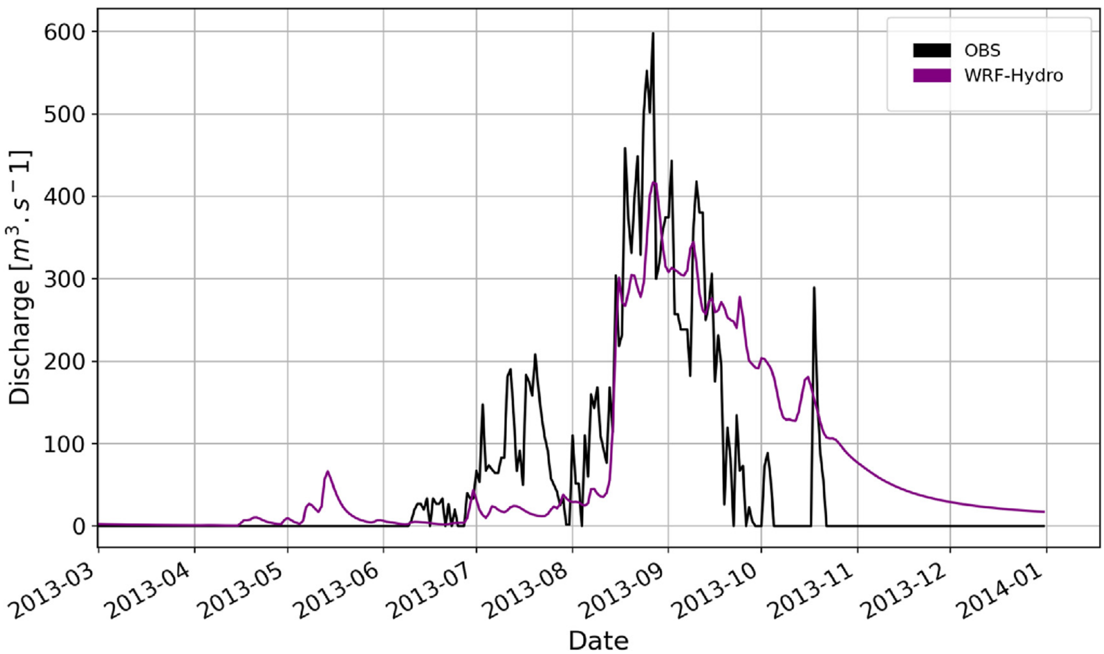

Figure 5. Validation of streamflow.

in Goronyo, and 35.92% in Bakolori while the simulation with the Ba scenario increased streamflow by 15.01% in Sokoto, 15.43% in Goronyo and 10.67% in Bakolori.

Figure 7 shows the daily differences between the streamflow from the control and each of the extreme LULCC scenarios for all the FPs. The pattern of change for all the FPs were almost the same in all the FPs with obvious changes in the monsoon season (i.e., June–September when we have high flows) and the least changes in the dry season. The built up scenario has very high increase in streamflow for all the FPs. Furthermore, the Ur scenario caused the highest increase in all the period. This could not be far from the fact that urban built-up lands has less infilteration capacity by creating impervious surface, removes vegetation and consequently removes transpiration as also shown in Figure 8b. This is in line with the work of Zhou (2014) which emphasized that increasing peak flow has been generally taken as the major hydrologic implication of urbanization. Also, almost all the upstream areas of Bakolori were converted into built up lands, and this could explain why we have much more higher percentage of increase in streamflow in this FP.

The effect of forest cover changes on mean streamflow is satisfactorily understood and data all over the world have revealed that increasing the forest cover of a catchment results into a decrease in the total volume of flow (Brown et al., 2013). Also, the rate of transpiration is generally different for various vegetation covers, as forested areas normally transpire at higher rates than shrubs and cultivated areas, hence could lead to a decreased streamflow. This could be confirmed from Figure 8, which shows a decrease in Evapotranspiration ET in all the period for the Ur and Ba scenarios with a subsequent increase in streamflow (Figure 7c) for Sokoto FP. However, the Fr scenario depicted an increase in ET (Figure 8) with a corresponding decrease in streamflow (Figure 7c) for Sokoto FP. Further analysis of the ET also clearly revealed that the contribution of

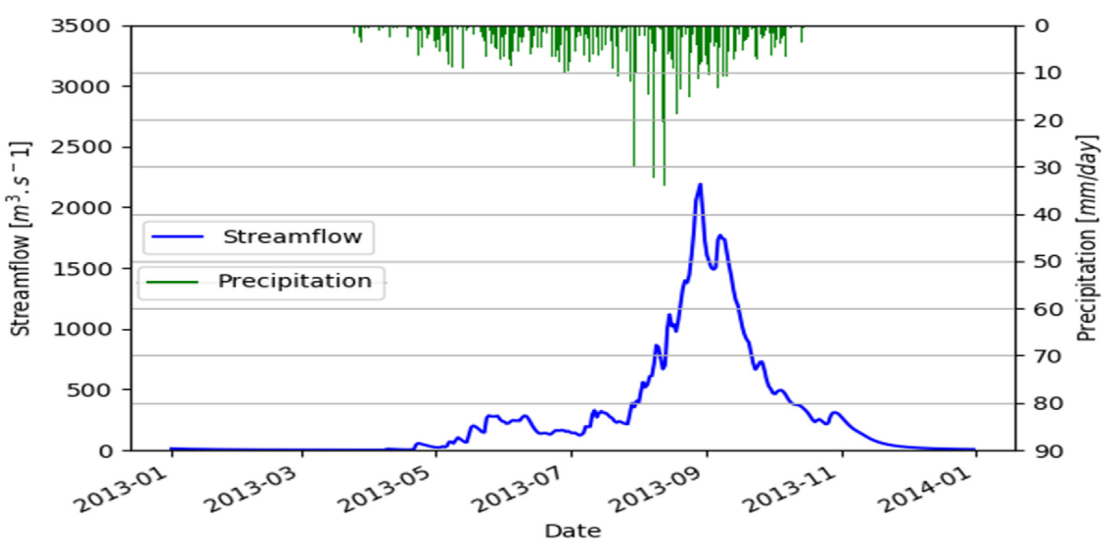

Figure 6. Variation of precipitation and streamflow over the entire basin (Sokoto).

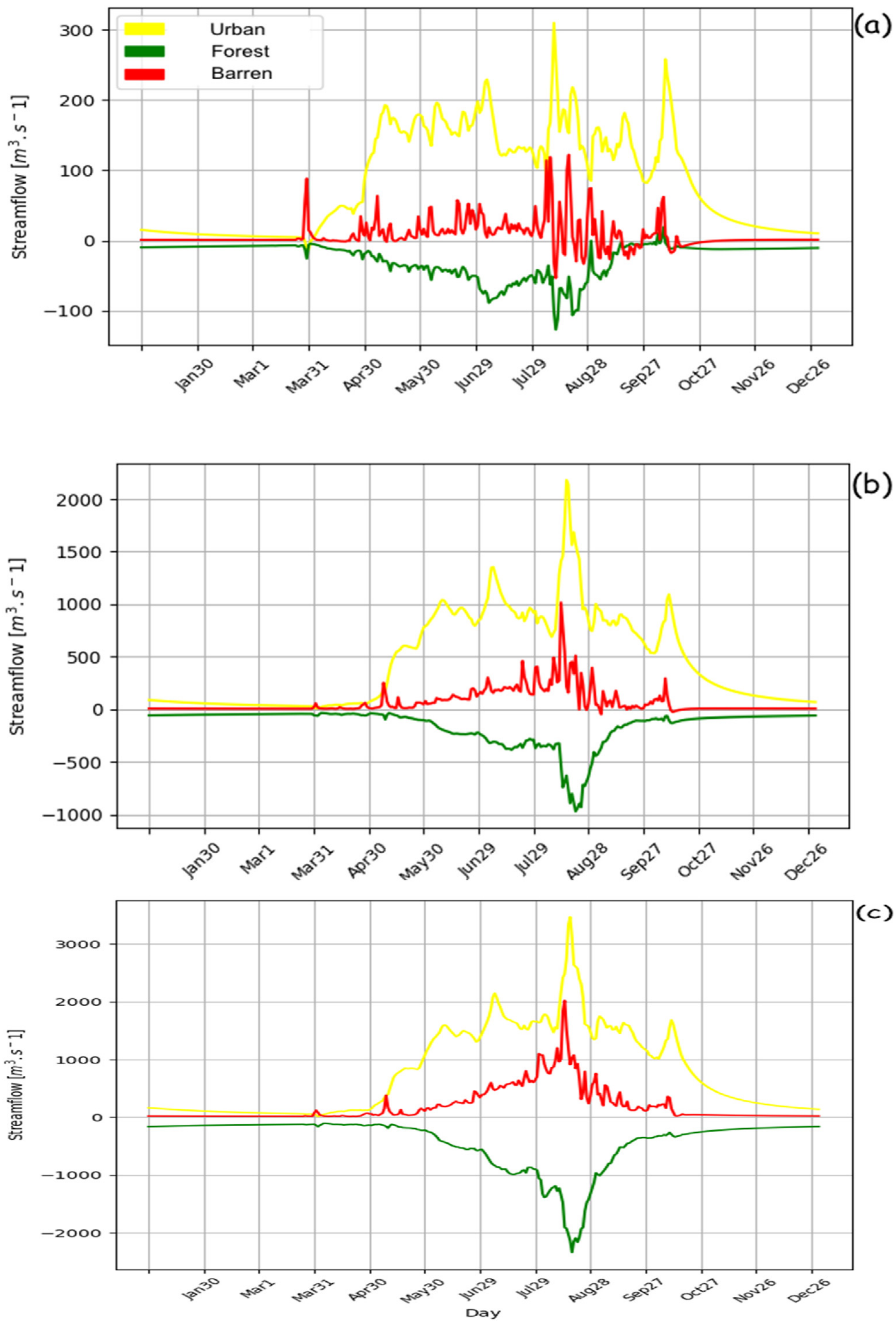

Figure 7. Daily Difference between the Control Streamflow and the extreme LULCC scenarios for (a) Bakolori, (b) Goronyo and (c) Sokoto Forecast Points.

transpiration to ET is quite higher for the Fr scenario than others. Also, as shown in Figure 8b, Fr scenario has a quite higher increase in transpiration than the other extreme scenarios because the deep roots can suck up more moisture from the soil; also deciduous forest has a larger leaf area for transpiration (Guo et al., 2008; Achugbu et al., 2021). Therefore, decrease in streamflow was due to intensified evapotranspiration for the afforested scenario as compared to the deforested scenario. This is in line with the Getahun and Van Lanen (2015) who revealed that 100% deforested extreme scenario showed higher streamflow and a decreased ET (Achugbu et al., 2021), while the 100% afforested scenario showed the opposite. Li et al. (2007) also revealed that overgrazing has a substantial impact on the water yield, as their result shows an increase ranging from 33% to 91% in streamflow increase for a 100% overgrazing scenario.

3.3. Comparison of the simulations from the LULCC scenarios

From Figure 9a-c, the mean of the control streamflow in Bakolori, Goronyo and Sokoto were closer to that of Sa and Gr but very far from that of Ur and Fr scenario. Also, the minimum and maximum flow was highest for the Bu and lowest for the Fr in all the forecast points. To

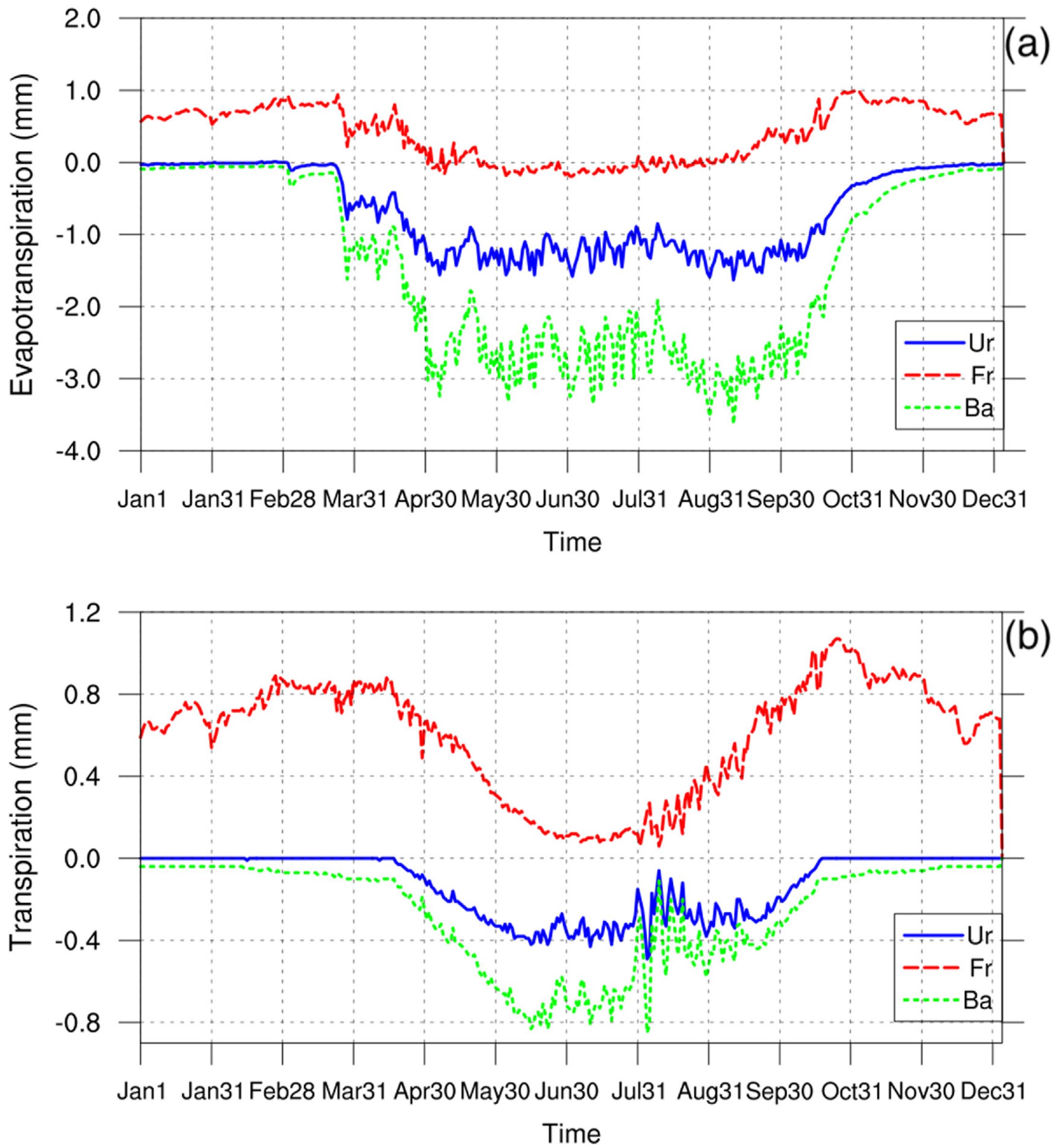

Figure 8. Daily Difference between the control streamflow and the extreme LULCC scenarios for Sokoto forecast point-controlled basin (i.e., the entire basin).

further compare the means of the simulations, a paired two-sample t-test was conducted. For Bakolori, the difference between the mean of the control and Ur, Sa, Fr and Ba were significant at 95% confidence level while that of Gr was not. For Goronyo, the difference between the mean of the control and Ur, Gr, Fr and Ba were significant at 95% confidence level while that of Sa was not. However, all the land use scenarios showed significant changes in streamflow at 95% confidence level for Sokoto, the entire basin.

Figure 9 reveals the minimum, maximum, mean and range values of the streamflow for all the FPs and ET for the entire basin. From Figure 9c and d, the comparison between simulated streamflow and the corresponding ET for the entire basin shows that there was a high evapotranspiration with the presence of forests than the control simulation, while the Ba scenario has the least ET. The reduction in ET for Ba when compared with the Ur could be attributed to the fact that there was more vegetation in the Ur scenario than for Ba.

From Table 4, the correlation between the input precipitation and the streamflow output for each LU scenario over the SRRB basin were strong with the urban having the strongest. Also, all the correlations were significant at level of $p < 0.05$ with the built up mostly significant. The mean SDR values for the LU scenarios in the SRRB with the corresponding p-value from the paired two-sample t-test between the control SDR and each land use scenario revealed that the Sa and Gr showed no statistically significant difference from the control SDR. However, a statistically significant different SDR was observed amidst the control and Ur, Fr and Ba scenarios. The mean SDR in the Ur scenario is the highest (49.2, $p = 0.017$) while the Fr has the lowest (14.6, $p = 0.05$).

3.4. Further analysis of Gr and Sa scenarios

Simulation with the Gr scenario have been shown to increase streamflow by about 1.33% in Sokoto, 1.62% in Goronyo and 0.23% in Bakolori for the entire year. The conversion of open shrublands into Savannas, croplands and cropland/natural vegetation mosaics into grasslands, results into increased vegetation coverage. This led to intensifying soil water storage and increasing the infilteration of rainfall into the basin, and by this means, increases the streamflow. Figure 10 also shows the monthly percentage change as the dry months generally show high percentage of decrease in streamflow. The scenario has the basin covered with about 98.8% grassland, which has very shallow roots

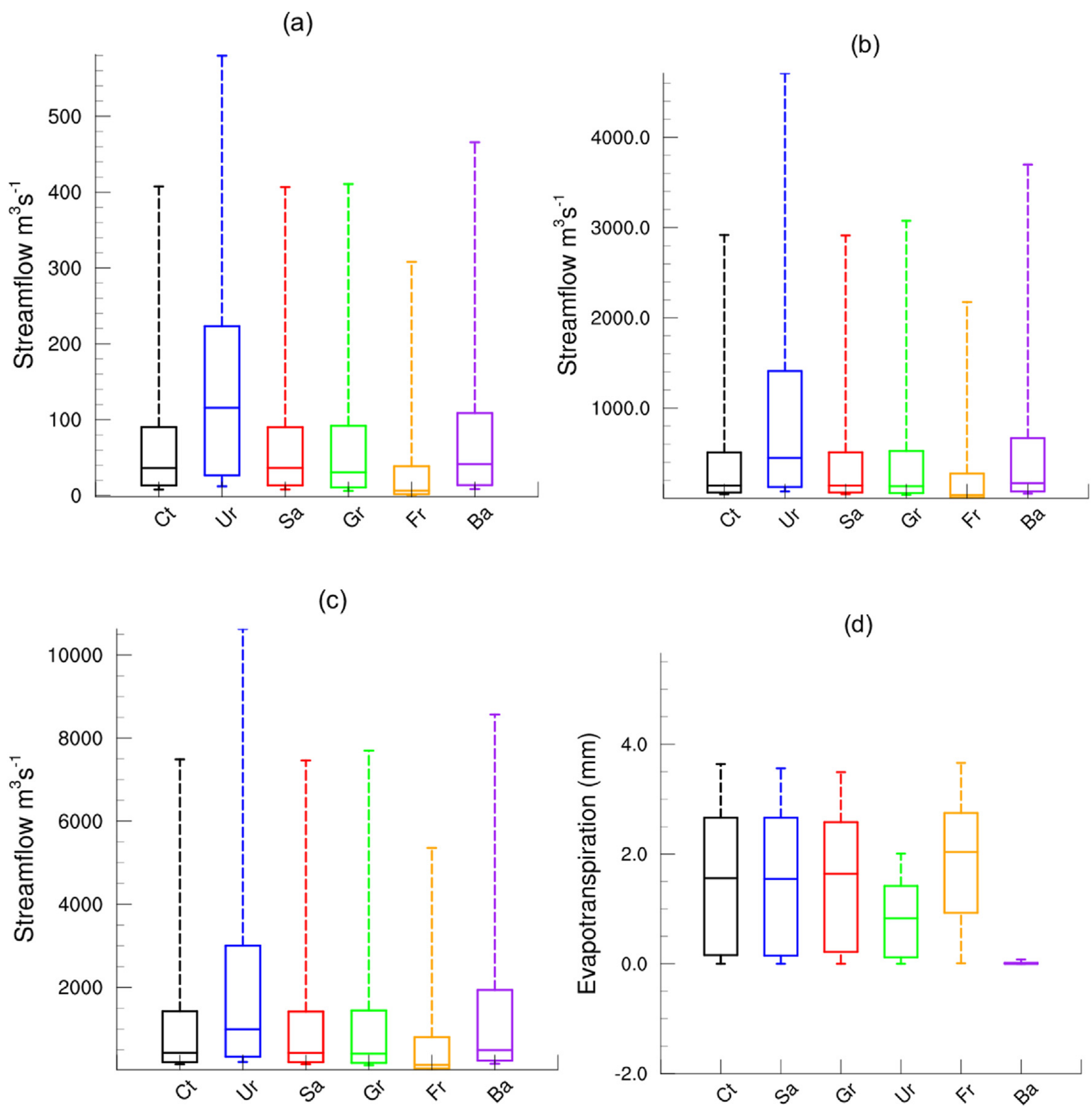

Figure 9. Streamflow for (a) Bakolori, (b) Goronyo and (c) Sokoto forecast points, and (d) Evapotranspiration for Sokoto basin.

and could be flooded during the monsoon season when there is heavy rainfall. This decreases the groundwater recharge and thereby increases the surface flow (Chakilu and Moges 2017; Gyamfi et al., 2017), and however decreases the surface flow in other months as the grasses wither as seen in Figure 10.

From the daily difference between the simulated streamflow from each LULCC scenario and the control simulation for the three forecast points (Figure 11), between July and October, the grassland scenario generally increased the streamflow. Researchers such as Dias et al. (2015), Neill et al. (2013), Panday et al. (2015), Souza-Filho et al. (2016) and Bekele et al. (2021) have all demonstrated that deforestation could lead to an increase in streamflow. Also, regards the differences during the wet (June–October) and dry (November–May) period over the basin, there was an increase in streamflow in the wet period and a decrease in the dry period for all the forecast points. Researchers like Kuchment (2008), Ogden et al. (2013), Liu et al. (2015), Guzha et al. (2018), Gebremicael et al. (2019), Kassie et al. (2019), Negese (2021) and Aredo et al. (2021) have all confirmed there is a reduction in streamflow during the dry season due to deforestation.

The conversion of grasslands into savannas (Sa) however, decreased streamflow by 0.09% in Sokoto, increased it in Goronyo by 0.01% and then increases in Bakolori by 0.24%. Cuo (2016), Zhang et al. (2017) and

Table 4. Pearson correlation between the input precipitation and the streamflow output, and the Specific Discharge to Rainfall ratios from each LU scenario over the SRRB basin.

	Control	Urban	Grassland	Savanna	Forest	Barren
Correlation coefficient	0.79**	0.90**	0.78**	0.79**	0.60*	0.84**
Mean SDR	22.00	49.20**	21.82	22.11	14.60**	25.09*

*, significant at a level of $p < 0.05$; **, significant at a level of $p < 0.01$.

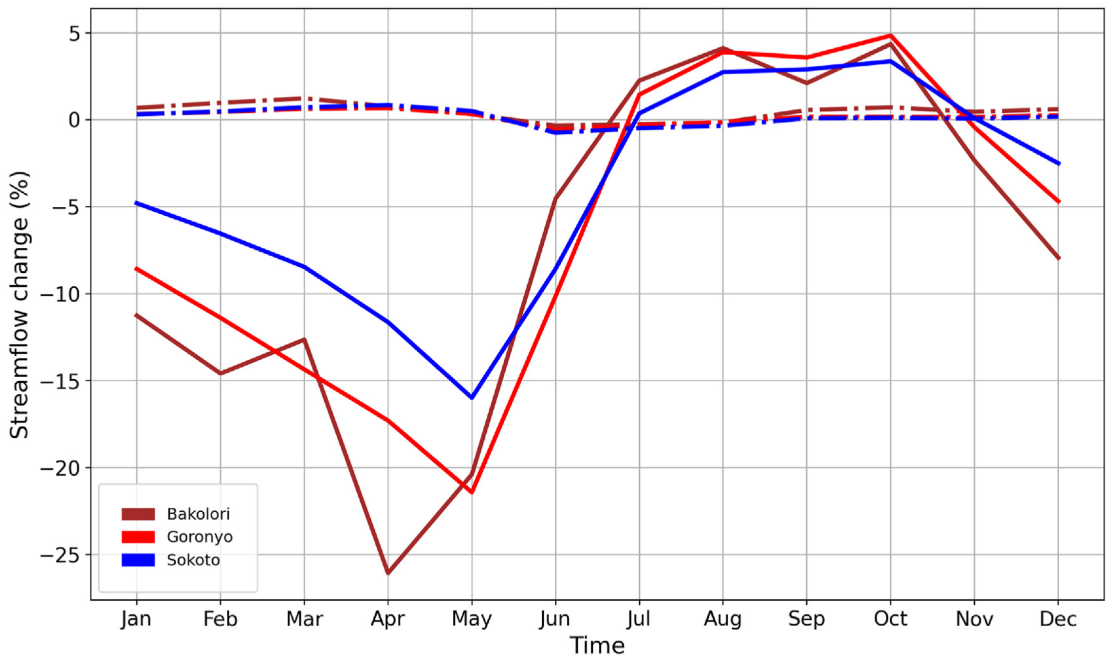

Figure 10. Monthly percentage change of in each Forecast Point for 2013 in the SRRB. Solid lines show the Gr scenarios, while the dashed lines show the Sr scenarios for each forecast point.

Takata and Hanasaki (2020) have demonstrated that afforestation has the capacity to decrease annual streamflow. The fact that the LCPs are not evenly distributed over the entire SRRB could be a good reason for the different response of the FPs to conversion from grasslands into savanna. According to Teuling et al. (2019), changes that take place at the sub-catchment level are many a times obscured by conflicting effect in other parts of the catchment. July to October is the period we generally have green grasses over the basin, after which they wither off.

It could also be seen from Figure 11 that the daily difference in streamflow increased from January until the end of May when it started decreasing. The decrease continued and became higher at the peak of the monsoon period in August, and then started increasing around the end of August, and continued throughout the remaining period of the year. Almost the same situation occurred in all the forecast points with just little variation, which could be attributed to the size/area of each basin, uneven LU parameters covering each basin/sub-basin and others. This shows that the size/area of the basin understudy is also a factor to be considered for a LULCC impact studies as basins with different sizes with same characteristics could have the tendency to behave differently, as seen in Sokoto (the largest), Goronyo and Bakolori (the smallest).

Researchers like Hurkmans et al. (2009), Wangpimool et al. (2013), have all confirmed that afforestation could cause an increase in dry season streamflow. Hundecha and Bardossy (2004) also deduced that an increase of peak and total runoff volume is the consequence of amplified land degradation and deforestation, which eventually decreases the availability of water, increases flood occurrence, and affects water quality (Gashaw et al., 2019; Aredehey et al., 2020). This analysis also showed that there was an increase in streamflow in the dry period for the Sa scenario while there was a decrease in the Gr scenario.

Figure 12 depicts the spatial distribution of the change in average ET due to LULCC for the Sa and Gr scenarios for the year. This is necessary to also explain how each FP was affected based on the level of LULCC that occurred as shown in Fig. 2c and d. It could be seen (from Figure 12a) that the areas with no alterations in LU parameter (as seen in Figure 2c) showed almost zero difference in evapotranspiration. This can also confirm that the sensitivity of the model to changes in LULCC could be reasonable. Also, the areas where grasslands were converted into savanna showed a little increase in evapotranspiration. The grasslands (dominated by herbaceous annuals with height less than 2m) were converted to savanna (which has about 10–30% tree coverage with greater than 2m height canopy coverage). The savanna has more deep rooted vegetation than the grasses, which has made it to have the ability to suck up more moisture from the soil. Therefore, decrease in streamflow could partly be due to the increase in ET for the Sa scenario in comparison with the Gr scenario. It also shows that afforestation could increase annual ET. This is compatible with the conclusion of Cuo (2016) and Zhang et al. (2017).

Strong correlation coefficients exist between the input precipitation and the output ET from each LU scenario over the entire basin wich is also significant for Ct, Sa and Gr (Huntington and Bilmire 2014). Researchers such as Nosetto et al. (2012), Warburton et al. (2012), Yira et al. (2016), Chemura et al. (2020) have stated that processes such as evapotranspiration, infiltration and percolation may change due to alterations of land cover type that can modify the water balance of a catchment. Evapotranspiration is a major component of the hydrologic process, at times nearly matching precipitation in the basin water balance, in which under a given climatic conditions, is mostly influenced by land cover (Schilling et al., 2008). With the same precipitation conditions, decline in ET gave rise to an increase in streamflow, while increased ET could cause a decrease (Hurkmans et al., 2009; Qin et al., 2017). Also, exchanging natural vegetation with pasture and cropland could be liable to the reduction of ET (Oliveira et al., 2014; Spera et al., 2016), which could be a pathway to streamflow increase (Brown et al., 2005). According to Guo et al. (2008), decrease in streamflow in forest area could be associated with increased water loss by evapotranspiration when compared with agricultural land.

However, the temporal daily ET difference between the control streamflow and the extreme LULCC scenarios for the entire basin (as shown in Figure 13a) revealed that the increase (decrease) in evapotranspiration due to LULCC is not linear with the afforestation (deforestation) scenario for the Sokoto FP. There was more ET for the PA scenario than the Gr scenario in the wet period, while there was more ET in the dry period for Gr than it is for the Sa scenario. In order to see some factors behind this, Figure 13b and c shows that bulk of the ET for the Sa scenario in the wet period came as a result of increased transpiration, while that of the Gr is mainly due to higher surface evaporation. It also

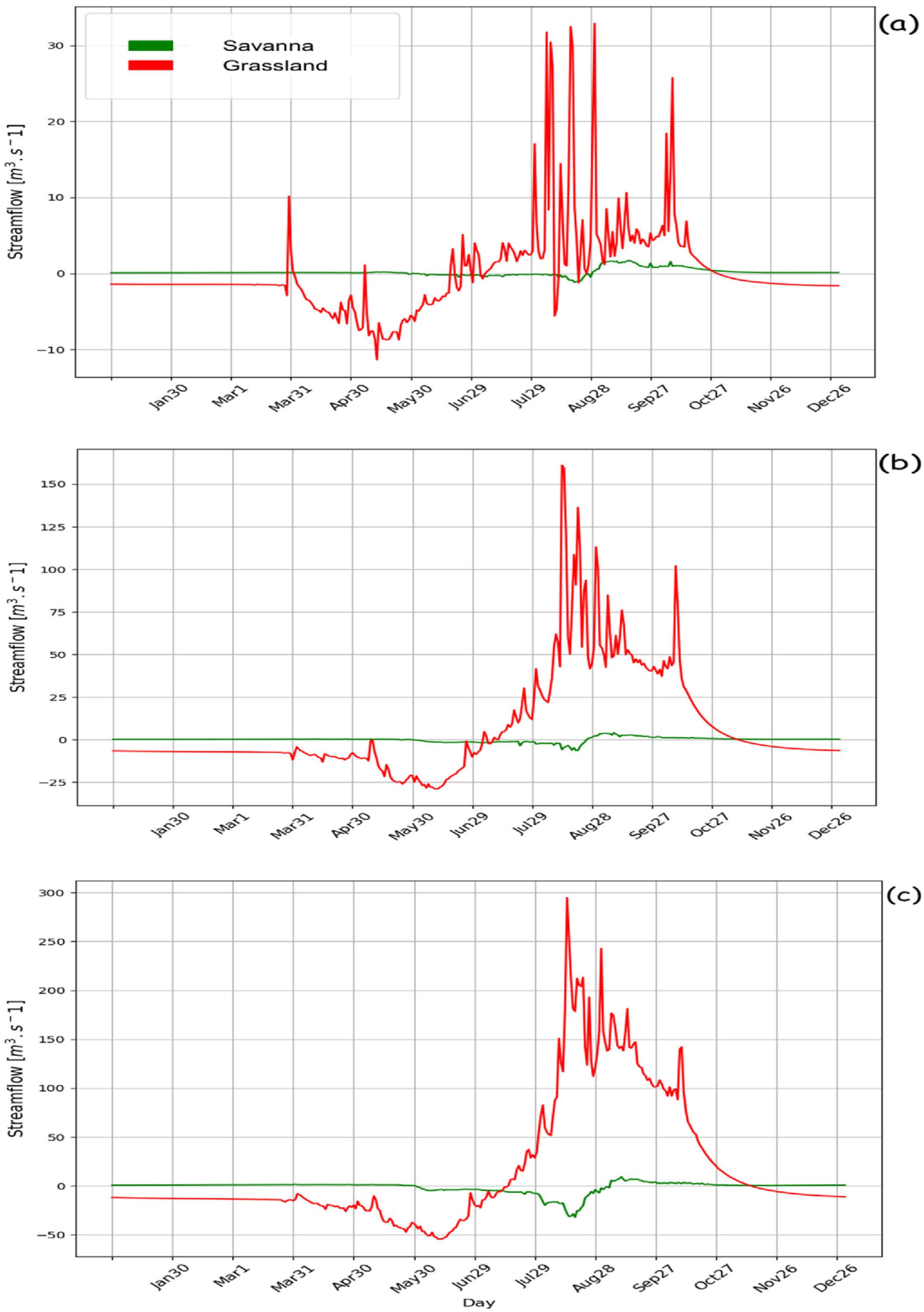

Figure 11. Daily Difference between the Control Streamflow and each Sa and Gr scenario for (a) Bakolori, (b) Goronyo and (c) Sokoto Forecast Points.

shows an increase in ET during the dry period when we have a decrease in streamflow for the Gr scenario, and a decrease in ET during the dry period when there was an increase in streamflow. Furthermore, there is a decrease in ET during the wet period when we have an increase in streamflow for the Gr scenario, and an increase in ET during the same period when we also have a decrease in streamflow. From Figure 13b, changes in transpiration were more obvious for both the wet and dry period with almost the same pattern of change with the ET, and this could mean that it has more influence than evaporation over the basin.

The partitioning of net radiation into Latent Heat (LH) and Sensible Heat (SH) fluxes can determine how wet the soil would be (Achugbu et al., 2020). This splitting up of surface energy critically depends on the

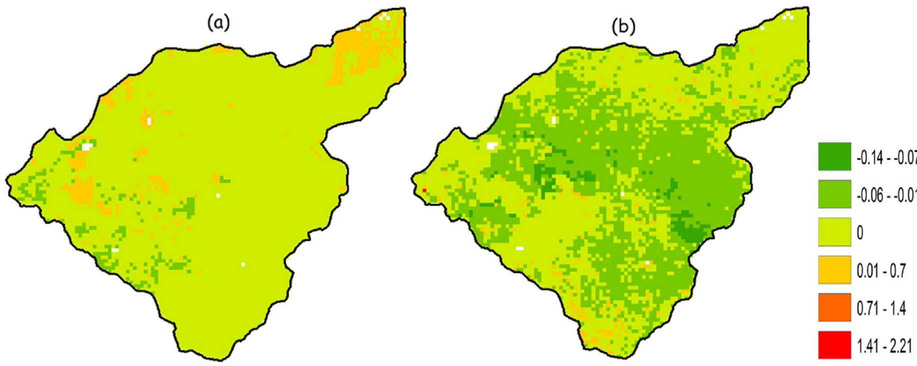

Figure 12. Spatial distribution of the difference between the control ET and (a) Sa and (b) Gr scenarios in mm/day.

moisture content of the soil (Klein et al., 2016). From Figure 13d, the Gr scenario shows clear impact of deforestation on the basin as there was an increase in LH during the dry period and a decrease during the wet period. This also reveals that more energy was partitioned into latent heat in the basin as a result of deforestation which could lead to more evapotranspiration during the dry season, and hence could worsen the problem of limited water prevailing in the basin especially during this period. The reduced LH in the wet period could be attributed to the fact that soil moisture plays a vital role in the partitioning of the surface energy. Figure 13e reveals that the Gr scenario averagely decreased the SH throughout the period. Furthermore, the Sa scenario caused a clear decrease in LH during the dry period, and an increase in SH throughout the period. This has the tendency to increase the surface temperature, increase evapotranspiration and cloud development, and leading to more precipitation and increased flow. However, other factors like advection and atmospheric circulation are strong factors that could also be at work.

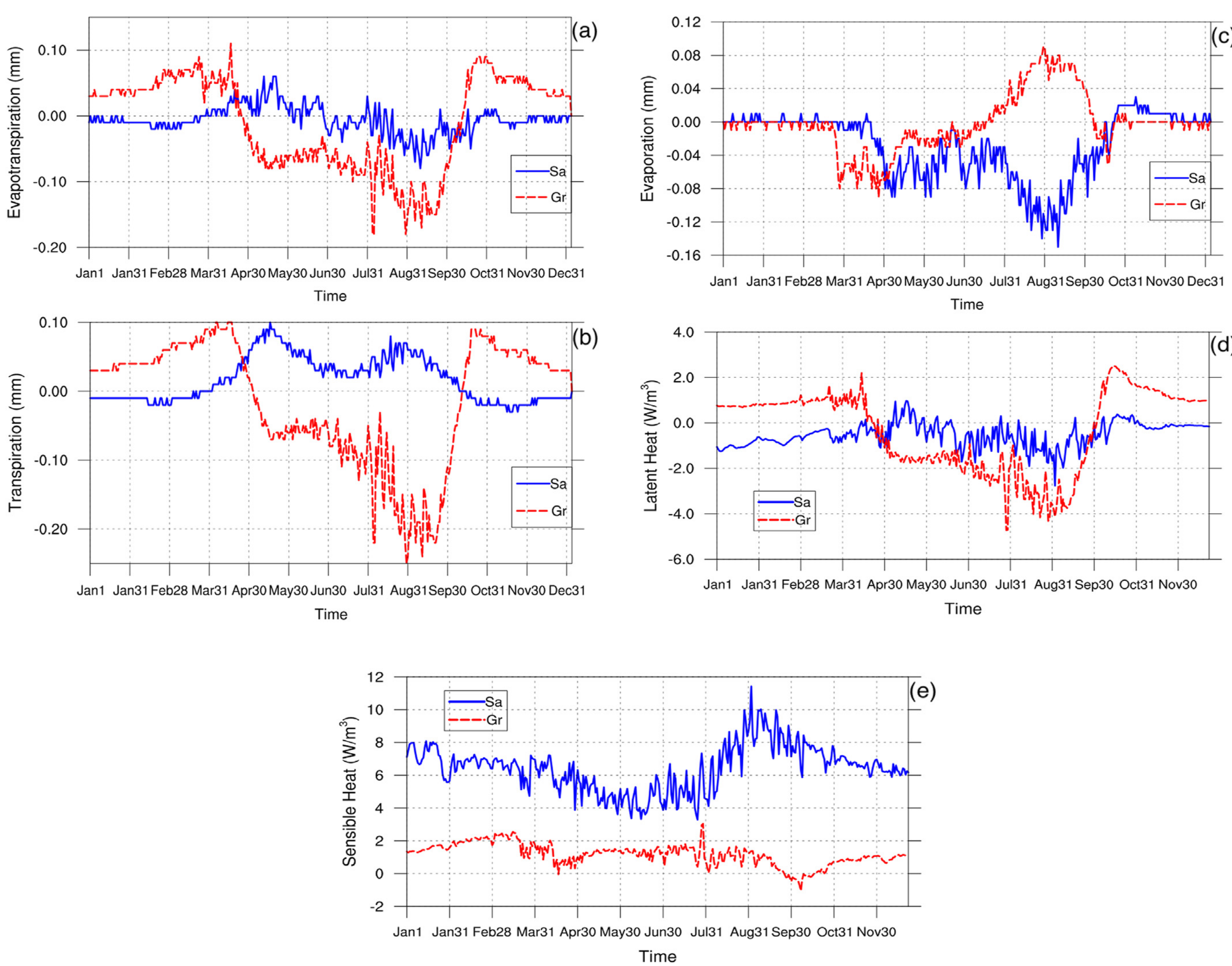

Figure 13. Daily Difference between the Control and each Sa and Gr scenario for Sokoto Forecast Point (i.e the entire basin).

Nevertheless, hydrologic response to land disturbance is highly nonlinear and variable, and is frequently influenced by a lot of abiotic and biotic factors, which includes climate, soils, vegetation characteristics and management practices (Sun et al., 2008). Therefore, there is a need for a long-term fields monitoring in order to better understand the basin's response to LULCC, as this will also help in getting a better calibration of the model. This demonstrates also that this kind of research is basin specific, although other factors like soil characteristics, atmospheric and some other hydrometeorological parameters which were not considered in this research could be at work. Also, uncertainties as regards the model set up and parameterisation combinations are strong factors that cannot be over-emphasised in LULCC impact studies. Hence, future work would be to run the simulation with several combination of land surface and boundary layer schemes in order to reduce uncertainties arising from that.

In general, streamflow was decreased due to afforestation during the wet season, which is a sign that the risk of river overflowing its bank would be reduced. This also indicates a reduction in the risk of flood occurrences in the basin as most flood events in the basin were as a result of river overflowing its bank at the peak of monsoon season.

4. Conclusion

In studying the response of streamflow to LULCC over the SRRB, WRF-Hydro model forced with WRF model outputs was used to run simulations with five different land cover scenarios generated for Urban (Ur), Savanna (Sa), Grassland (Gr), Forest (Fr) and Barren (Ba). WRF-Hydro model was calibrated and validated by adjusting the infiltration parameter as well as Manning's roughness parameter in the model. Result showed that the model could be used for hydrometeorological studies in the basin as it could replicate the observed streamflow reasonably well. The discussion of the LULCC effect on streamflow was accentuated on the Sa and the Gr scenarios.

For the extreme scenario simulation, the Ur scenario increased the streamflow by 59.21% in Sokoto, 104.15% in Goronyo and 117.08% in Bakolori. The Fr scenario decreased the streamflow by 31.47% in Sokoto, 35.12% in Goronyo, and 35.92% in Bakolori while the simulation with the Ba scenario increased streamflow by 15.01% in Sokoto, 15.43% in Goronyo and 10.67% in Bakolori.

Simulation with the Gr scenario have been shown to increase streamflow by about 1.33% in Sokoto, 1.62% in Goronyo and 0.23% in Bakolori, while the conversion of grasslands into savannas (Sa) decreased streamflow by 0.03% in Sokoto, increased it in Goronyo by 0.15% and then increases in Bakolori by 0.46%. Further analysis showed an increase in streamflow in the dry period due to afforestation and a decrease due to deforestation. The Sa scenario also showed a decrease in streamflow during the wet period while the Gr scenario showed an increase. Areas where grasslands were converted into savanna showed a little increase in evapotranspiration. Consequently, decrease in streamflow could partly be due to increased ET for the Sa scenario as compared to the Gr scenario, but have been shown to be nonlinear.

There was more ET for the Sa scenario than the Gr scenario in the wet period, while there was more ET in the dry period for Gr scenario than it is for the Sa scenario. Notwithstanding, other factors like soil characteristics, atmospheric and some other hydrometeorological parameters which could not be considered in this research may be at work, the research have shown that LULCC can affect the streamflow over the SRRB which is a very important basin as it provides portable water for domestic use and for agriculture in a semi-arid and water scarce environment. The combination of remote sensing, GIS and WRF-Hydro model provides a functional approach in evaluating the impact of LULCC on catchment hydrology, which is essential in the selection, and development of workable basin management options which would promote sustainable use of land and water resources. However, based on the research findings, the Nigeria and Niger government needs to be energetic in creating policies for appropriate LU management over the basin. Further work is recommended to capture all the area of the SRRB to have a better evaluation of LULCC impacts on the basin. Also, incorporation of high-resolution satellite data like LANDSAT and SPOT is recommended for future work so as to capture small-scale phenomena, which the after-match effect could be significant. Catchment stakeholders and policy makers would use the outcomes of this research to tackle the issues arising from catchment deterioration. This research will also help in making informed decisions in the selection and development of feasible catchment management choices to ensure sustainable use of land and water resources within the SSRB. The study revealed that the sensitivity of WRF-Hydro to LULCC is reasonable. However, more research is needed to compare outputs from same basin with different hydrological model popularly used for LULCC impact studies. Future work would also include running the forcing data simulation with several combination of land surface and boundary layer schemes in order to reduce uncertainties arising from model set up and parameterisation combinations.

Declarations

Author contribution statement

Ifeanyi Chukwudi Achugbu: Conceived and designed the experiments; Performed the experiments; Analyzed and interpreted the data; Contributed reagents, materials, analysis tools or data; Wrote the paper.

Ayo Akinlabi Olufayo; Ifeoluwa Adebowale Balogun; Jimy Dudhia & Elijah Adesanya Adefisan: Contributed reagents, materials, analysis tools or data.

Molly McAllister: Performed the experiments; Analyzed and interpreted the data.

Edward Naabil: Contributed reagents, materials, analysis tools or data; Performed the experiments.

Funding statement

This research did not receive any specific grant from funding agencies in the public, commercial, or not-for-profit sectors.

Data availability statement

Data will be made available on request.

Declaration of interests statement

The authors declare no conflict of interest.

Additional information

No additional information is available for this paper.

Acknowledgements

We express our gratitude to the Mesoscale and Microscale Meteorology (MMM) Laboratory and the Research Applications Laboratory (RAL) in NCAR for supporting the research, and also acknowledge the NCAR's Computational and Information System Laboratory for making available the computing facilities used in this research. Many thanks to Katelyn FitzGerald, Mike Dixon, David Gochis, Micheal Duda, and other NCAR staff for their support. Also, many thanks to the Sokoto Rima River Basin Development Authority (SRRBDA) for providing the streamflow data used for the model calibration. The German Federal Ministry of Education and Research (BMBF) primarily funded the research work via WACS-GRP FUTA.

Appendix 1. International Geosphere-Biosphere Programme legend and class descriptions

Name	Value	Description
Evergreen Needleleaf Forests (EN)	1	Dominated by evergreen conifer trees (canopy >2m) Tree cover >60%
Evergreen Broadleaf Forests (EB)	2	Dominated by evergreen broadleaf and palmate trees (canopy >2m) Tree cover >60%
Deciduous Needleleaf Forests (DN)	3	Dominated by deciduous needleleaf (larch) trees (canopy >2m) Tree cover >60%
Deciduous Broadleaf Forests (DB)	4	Dominated by deciduous broadleaf trees (canopy >2m) Tree cover >60%
Mixed Forests (Mf)	5	Dominated by neither deciduous nor evergreen (40–60% of each) tree type (canopy >2m) Tree cover >60%
Closed Shrublands (Cs)	6	Dominated by woody perennials (1–2m height) > 60% cover
Open Shrublands (Os)	7	Dominated by woody perennials (1–2m height) 10–60% cover
Woody Savannas (Ws)	8	Tree cover 30–60% (canopy >2m)
Savannas (Sa)	9	Tree cover 10–30% (canopy >2m)
Grasslands (Gr)	10	Dominated by herbaceous annuals (<2m)
Permanent Wetlands (Pw)	11	Permanently inundated lands with 30–60% water cover and >10% vegetated cover
Croplands (Cr)	12	At least 60% of area is cultivated cropland
Urban and Built-up Lands (Ub)	13	At least 30% impervious surface area including building materials, asphalt, and vehicles
Cropland/Natural Vegetation Mosaics (Cv)	14	Mosaics of small-scale cultivation 40–60% with natural tree, shrub, or herbaceous vegetation
Permanent Snow and Ice (Ps)	15	At least 60% of area is covered by snow and ice for at least 10 months of the year
Barren (Br)	16	At least 60% of area is non-vegetated barren (sand, rock, soil) areas with less than 10% vegetation
Water Bodies (Wb)	17	At least 60% of area is covered by permanent water bodies
Unclassified	255	Has not received a map label because of missing inputs

Adapted from Sulla-Menashe and Friedl (2018), modified by Achugbu et al., 2021.

References

Abdullahi, S.A., Muhammad, M.M., Adeogun, B.K., Mohammed, I.U., 2014. Assessment of water availability in the Sokoto Rima River Basin. Res. Environ. 4 (5), 220–233.

Aboelnour, M., Gitau, M.W., Engel, B.A., 2020. A comparison of streamflow and baseflow responses to land-use change and the variation in climate parameters using SWAT. Water 12 (1), 191.

Achugbu, I.C., Dudhia, J., Olufayo, A.A., Balogun, I.A., Adefisan, E.A., Gbode, I.E., 2020. Assessment of WRF land surface model performance over West Africa. Adv. Meteorol., 6205308

Achugbu, I.C., Olufayo, A.A., Balogun, I.A., Adefisan, E.A., Dudhia, J., Naabil, E., 2021. Modeling the spatiotemporal response of dew point temperature, air temperature and rainfall to land use land cover change over West Africa. Model. Earth Syst. Environ. 8, 173–198.

Aduah, M.S., Jewitt, G.P.W., Toucher, M.L.W., 2017. Assessing impacts of land use changes on the hydrology of a lowland rainforest catchment in Ghana. West Afr. Water 10 (9), 1–15.

Akpoti, K., Antwi, E.O., Kabo-bah, A.T., 2016. Impacts of rainfall variability, land use and land cover change on stream flow of the black volta basin. West Afr. Hydrol. 3 (26), 1–24.

Alemayehu, K.T., 2015. Land use land cover change and its implication on surface runoff: a Case study of baro River Basin in south western Ethiopia. J. Environ. Earth Sci. 5 (8).

Aredehey, G., Mezgebu, A., Girma, A., Li, F., 2020. The effects of land use land cover change on hydrological flow in Giba catchment, Tigray, Ethiopia. Cogent Environ. Sci. 6 (1), 1785780.

Aredo, M.R., Hatiye, S.D., Pingale, S.M., 2021. Impact of land use/land cover change on stream flow in the Shaya catchment of Ethiopia using the MIKE SHE model. Arabian J. Geosci. 14, 114.

Armitage, P.D., Petts, G.E., 1992. Biotic score and prediction to assess the effects of water abstractions on river macroinvertebrates for conservation purposes. Aquat. Conserv. Mar. Freshw. Ecosyst. 2 (1), 1–17.

Bartzen, B.A., Dufour, K.W., Clark, R.G., Caswell, F.D., 2010. Trends in agricultural impact and recovery of wetlands in prairie Canada. Ecol. Appl. 20, 525–538.

Bekele, D., Alamirew, T., Kebede, A., Zeleke, G., Melesse, A.M., 2021. Modeling the impacts of land use and land cover dynamics on hydrological processes of the Keleta watershed, Ethiopia. Sustain. Environ. 7 (1), 1–14.

Belward, A.S., Estes, J.E., Kline, K.D., 1999. The igbp-dis global 1-km land-cover data set discover. Proj. Overview Photogram. Eng. Remote Sens. 65 (9), 1013–1020.

Brown, A.E., Western, A.W., McMahon, T.A., Zhang, L., 2013. Impact of forest cover changes on annual streamflow and flow duration curves. J. Hydrol. 483, 39–50.

Brown, A.E., Zhang, L., McMahon, T.A., Western, A.W., Vertessy, R.A., 2005. A review of paired catchment studies for determining changes in water yield resulting from alterations in vegetation. J. Hydrol. 310 (1–4), 28–61.

Burbank, D.W., Bookhagen, B., Gabet, E.J., Putkonen, J., 2012. Modern climate and erosion in the Himalaya C. R Geosci. 344, 610–626.

Carrington, D.P., Gallimore, R.G., Kutzbach, J.E., 2001. Climate sensitivity to wetlands and wetland vegetation in mid-holocene north Africa. Clim. Dynam. 17, 151–157.

Case, J.L., LaFontaine, F.J., Kumar, S.V., Peters-Lidard, C.D., 2012. Using the NASA-Unified WRF to assess the impacts of real-time vegetation on simulations of severe weather Preprints. In: 13th Annual WRF User's Workshop Boulder CO, p. 69.

Chakilu, G.G., Moges, M.A., 2017. Assessing the land use/cover dynamics and its impact on the low flow of gumara watershed, upper blue nile basin Ethiopia. Hydrol. Curr. Res. 7, 268.

Chemura, A., Rwasoka, D., Mutanga, O., Dube, T., Mushore, T., 2020. The impact of land-use/land cover changes on water balance of the heterogeneous Buzi sub-catchment. Zimb. Rem. Sens. Appl.: Soc. Environ. 18, 100292.

Croke, B.F.W., Merritt, W.S., Jakeman, A.J., 2004. A dynamic model for predicting hydrologic response to land cover changes in gauged and ungauged catchments. J. Hydrol. 291, 115–131.

Cuo, L., 2016. In: Tang, Q., Oki, T. (Eds.), Land Use/cover Change Impacts on Hydrology in Large River Basins: A Review Terrestrial Water Cycle and Climate Change—Natural and Human-Induced Impacts. American Geophysical Union, Wiley, (Washington DC, USA, pp. 103–134.

Dee, D.P., Uppala, S.M., Simmons, A.J., Berrisford, P., Poli, P., Kobayashi, S., Andrae, U., Balmaseda, M., Balsamo, G., Bauer, P., Bechtold, P., Beljaars, C.M., 2011. The ERA-Interim reanalysis: configuration and performance of the data assimilation system. Q. J. R. Meteorol. Soc. 137 (656), 553–597.

Dias, L.C.P., Macedo, M.N., Costa, M.H., Coe, M.T., Neill, C., 2015. Effects of land cover change on evapotranspiration and streamflow of small catchments in the Upper Xingu River Basin, Central Brazil. J. Hydrol.: Reg. Stud. 4 (Part B), 108–122.

Ekoh, H.C., 2020. Analysis of Rainfall Trend in Sokoto State, Nigeria (1987-2016), 28. World News of Natural Sciences, pp. 171–186.

Ekpoh, I.J., Ekpenyong, Nsa, FRGS, 2011. The effects of recent climatic variations on water yield in the Sokoto region of northern Nigeria. Int. J. Bus. Soc. Sci. 2 (7) [Special Issue –April 2011 Netherlands Environmental Assessment Agency, 2005, The Effects of Climate Change in the Netherlands.

Foley, J.A., DeFries, R., Asner, G.P., Barford, C., Bonan, G., Carpenter, S.R., Chapin, F.S., Coe, M.T., Daily, G.C., Gibbs, H.K., Helkowski, J.H., Holloway, T., Howard, E.A., Kucharik, C.J., Monfreda, C., Patz, J.A., Prentice, I.C., Ramankutty, N., Snyder, P.K., 2005. Global consequences of land use science. Science 309, 570–574.

Gashaw, T., Tulu, T., Argaw, M., Worqlul, A.W., 2019. Modeling the impacts of land use–land cover changes on soil erosion and sediment yield in the Andassa watershed, upper Blue Nile basin, Ethiopia. Environ. Earth Sci. 78 (24), 679.

Gbode, I.E., Dudhia, J., Ogunjobi, K.O., Ajayi, V.O., 2018. Sensitivity of different physics schemes in the WRF model during a West African monsoon regime. Theor. Appl. Climatol. 136, 733–751.

Gebremicael, T.G., Mohamed, Y.A., Van der Zaag, P., 2019. Attributing the hydrological impact of different land use types and their long-term dynamics through combining parsimonious hydrological modelling, alteration analysis and PLSR analysis. Sci. Total Environ. 660, 1155–1167.

Getahun, Y.S., Van Lanen, H.A.J., 2015. Assessing the impacts of land use-cover change on hydrology of melka kuntrie subbasin in Ethiopia, using a conceptual hydrological model. Hydrol. Curr. Res. 6, 210.

Gochis, D.J., Barlage, M., Dugger, A., FitzGerald, K., Karsten, L., McAllister, M., McCreight, J., Mills, J., RafieeiNasab, A., Read, L., Sampson, K., Yates, D., Yu, W., 2018. The WRF-Hydro Modeling System Technical Description, (Version 50) NCAR Technical Note 107 Pages Available Online at:. https://ralucaredu/sites/default/files/public/WRFHydroV5TechnicalDescriptionpdf.

Guo, H., Qi, Hu, Jiang, Tong, 2008. Annual and seasonal stream ow responses to climate and land-cover changes in the Poyang Lake basin China. J. Hydrol. 355 (1-4), 106–122.

Gupta, H.V., Kling, H., Yilma, K.K., Martinez, G.F., 2009. Decomposition of the mean squared error and NSE performance criteria: implications for improving hydrological modeling. J. Hydrol. 377, 80–91.
Guzha, A.C., Rufino, M.C., Okoth, S., Jacobs, S., Nóbrega, R.L.B., 2018. Impacts of land use and land cover change on surface runoff, discharge and low flows: evidence from East Africa. J. Hydrol.: Reg. Stud. 15, 49–67.
Gyamfi, C., Ndambuki, J.M., Anornu, G.K., Kifanyi, G.E., 2017. Groundwater recharge modelling in a large-scale basin: an example using the SWAT hydrologic model. Model Earth Syst. Environ.
Hong, S.Y., Lim, J.O.J., 2006. The WRF single-moment 6-class microphysics scheme (WSM6). J. Korean Meteor. Soc. 42, 129–151.
Hundecha, Y., Bardossy, A., 2004. Modeling of the effect of land use changes on the runo generation of a river basin through parameter regionalization of a watershed model. J. Hydrol. 292 (1–4), 281–295.
Huntington, T.G., Bilmire, M., 2014. Trends in precipitation, runoff, and evapotranspiration for rivers draining to the gulf of Maine in the United States. J. Hydrometeorol. 15 (2), 726–743.
Hurkmans, R.T.W.L., Terink, W., Uijlenhoet, R., Moors, E.J., Torch, P.A., et al., 2009. Effects of land use changes on streamflow generation in the Rhine basin. Water Resour. Res. 45, 1–15.
Iacono, M.J., Delamere, J.S., Mlawer, E.J., Shephard, M.W., Clough, S.A., Collins, W.D., 2008. Radiative forcing by long-lived greenhouse gases: calculations with the AER radiative transfer models. J. Geophys. Res. 113 (D13103).
Jones, A.D., Calvin, K.V., Collins, W.D., Edmonds, J., 2015. Accounting for radiative forcing from albedo change in future global land-use scenarios. Clim. Change 131, 691–703.
Kannan, N., Santhi, C., White, M.J., Mehan, S., Arnold, J.G., Gassman, P.W., 2019. Some challenges in hydrologic model calibration for large-scale studies: a Case study of SWAT model application to Mississippi-atchafalaya River Basin. Hydrology 6 (17).
Kassie, A.E., Tesema, T.A., Amencho, N.W., 2019. Evaluation of stream flow under land use land cover change: a case study of Chemoga Catchment, Abay Basin Ethiopia. Afr. J. Environ. Sci. Technol. 14 (1), 26–39.
Khoi, D.N., Loi, P.T., Sam, T.T., 2021. Impact of future land-use/cover change on streamflow and sediment load in the Be River Basin. Vietnam. Water 13 (9), 1244.
Klein, C., Bliefernicht, J., Heinzeller, D., Gessner, U., Klein, I., Kunstmann, H., 2016. Feedback of observed interannual vegetation change: a regional climate model analysis for the West African monsoon. Clim. Dynam. 48 (9-10), 2837–2858.
Kuchment, L.S., 2008. Runoff Generation (Genesis, Models, Prediction) Water Problems Institute of RAN 394.
Kumar, N., Singh, S.K., Singh, V.G., Dzwairo, B., 2018. Investigation of impacts of land use/land cover change on water availability of Tons River Basin, Madhya Pradesh, India. Model. Earth Syst. Environ. 4, 295–331.
Lal, R., 1997. Deforestation and land-use effects on soil degradation and rehabilitation in western Nigeria IV hydrology and water quality. Land Degrad. Dev. 8, 95–126.
Li, K.Y., Coe, M.T., Ramankutty, N., De Jong, R., 2007. Modeling the hydrological impact of land-use change in West Africa. J. Hydrol. 337, 258–268.
Li, X., Mitra, C., Dong, L., Yang, Q., 2018. Understanding land use change impacts on microclimate using Weather Research and Forecasting (WRF) model. Phys. Chem. Earth 103, 115–126.
Liu, W., Wei, X., Fan, H., Guo, X., Liu, Y., Zhang, M., Li, Q., 2015. Response of flow regimes to deforestation and reforestation in a rain-dominated large watershed of subtropical China. Hydrol. Process. 29, 5003–5015.
Loveland, T.R., Belward, A.S., 1997. The international geosphere biosphere programme data and information system global land cover data set (DISCover). Acta Astronaut. 41 (4), 681–689.
Ma, Y., Chandrasekar, V., Chen, H., Cifelli, R., 2021. Quantifying the potential of AQPI gap-filling radar network for streamflow simulation through a WRF-hydro experiment. J. Hydrometeorol. 22 (7), 1869–1882.
Merritt, W.S., Letcher, R.A., Jakeman, A.J., 2003. A review of erosion and sediment transport models. Environ. Model. Software 18, 761–799.
Naabil, E., Lamptey, B.L., Arnault, J., Olufayo, A., Kunstmann, H., 2017. Water resources management using the WRF-Hydro modelling system : Case-study of the Tono dam in West Africa Journal of Hydrology. Reg. Stud. 12, 196–209.
Nakanishi, M., Niino, H., 2006. An Improved Mellor–Yamada level-3 model: its numerical stability and application to a regional prediction of advection fog. Bound-Layer Meteor. 119, 397–407.
Nash, J.E., Sutcliffe, J.V., 1970. River flow forecasting through conceptual models, 1 A discussion of principles. J. Hydrol. 10, 282–290.
Negese, A., 2021. Impacts of land use and land cover change on soil erosion and hydrological responses in Ethiopia. Appl. Environ. Soil Sci. 2021. Article ID 6669438, 10 pages.
Neill, C., Coe, M.T., Riskin, S.H., Krusche, A.V., Elsenbeer, H., Macedo, M.N., et al., 2013. Watershed responses to Amazon soya bean cropland expansion and intensification. Phil. Trans. Roy. Soc. Lond. B 368 (1619), 20120425.
Ngana, J.O., 2002. Integrated water resources management: the Case of the pangani River Basin. In: Ngana, J.O. (Ed.), Water Resources Management in the Pangani River Basin: Challenges and Opportunities Dar Es Salaam. Dar es Salaam University Press, 1 – 8.
Niu, G.-Y., Yang, Z.-L., Mitchell, K.E., Chen, F., Ek, M.B., Barlage, M., Longuevergne, L., Kumar, A., Manning, K., Niyogi, D., Rosero, E., Tewari, M., Xia, Y., 2011. The community Noah land surface model with multiparameterization options (Noah-MP): 1 Model description and evaluation with local-scale measurements. J. Geophys. Res. 116 (D12109).
Nosetto, M.D., Jobbágy, E.G., Brizuela, A.B., Jackson, R.B., 2012. The hydrologic consequences of land cover change in central Argentina Agric Ecosyst. Environ. Times, 154 2–11.
Ogden, F.L., Crouch, T.D., Stallard, R.F., Hall, J.S., 2013. Effect of land cover and use on dry season river runoff, runoff efficiency, and peak storm runoff in the seasonal tropics of Central Panama. Water Resour. Res. 49, 8443–8462.
Ohana-Levi, N., Karnieli, A., Egozi, R., Givati, A., Peeters, A., 2015. Modeling the Effects of Land-Cover Change on Rainfall-Runoff Relationships in a Semiarid, Eastern Mediterranean Watershed, 2015. Hindawi Publishing Corporation Advances in Meteorology. Article ID 838070, 16 pages.
Oliveira, P., Nearing, M., Moran, M., Goodrich, D., Wendland, E., Gupta, H., 2014. Trends in water balance components across the Brazilian Cerrado. Water Res. Res. 50 (9), 7100–7114.
Panday, P.K., Coe, M.T., Macedo, M.N., Lefebvre, P., Castanho, A.D. d A., 2015. Deforestation offsets water balance changes due to climate variability in the Xingu River in eastern Amazonia. J. Hydrol. 523, 822–829.
Patil NS, Nataraja M. (2020) Effect of land use land cover changes on runoff using hydrological model: a case study in Hiranyakeshi watershed. Model Earth Syst. Environ. 6, 2345–2357.
Pereira, H.C., 1989. Policy and Practice of Water Management in Tropical Areas. Westview Press, Boulder, Co.
Pitman, A.J., 2003. The evolution of, and revolution in, land surface schemes designed for climate models. Int. J. Climatol. 23, 479–510.
Qin, J., Ding, Y., Han, T., Liu, Y., 2017. Identification of the factors influencing the baseflow in the permafrost region of the northeastern qinghai-tibet plateau. Water 9 (9), 666.
Savenije, H.H.G., 1995. New definitions for moisture recycling and the relation with land use changes in the Sahel. H Hydrol. 167, 57–78.
Schilling, K.E., Jha, M.K., Zhang, Y.-K., Gassman, P.W., Wolter, C.F., 2008. Impact of land use and land cover change on the water balance of a large agricultural watershed: historical effects and future directions. Water Resour. Res. 44 (7), W00A09.
Sertel, E., Ormeci, C., Robock, A., 2011. Modelling land cover change impact on the summer climate of the Marmara Region, Turkey. Int. J. Glob. Warming 3 (1/2), 194–202.
Shuster, W.D., Bonta, J., Thurston, H., Warnemuende, E., Smith, D.R., 2005. Impacts of impervious surface on watershed hydrology: a review. Urban Water J. 2 (4), 263–275.
Souza-Filho, P.W.M., de Souza, E.B., Silva, R.O., Silva Júnior, R.O., Nascimento Jr., W.R., Versiani de Mendonça, B.R., et al., 2016. Four decades of land-cover, land-use and hydroclimatology changes in the Itacaiúnas River watershed, southeastern Amazon. J. Environ. Manag. 167, 175–184.
Spera, S., Galford, G., Coe, M., Macedo, M., Mustard, J., 2016. Land-use change affects water recycling in Brazil's last agricultural frontier. Global Change Biol. 22 (10).
Sulla-Menashe, D., Friedl, M.A., 2018. User Guide to Collection 6 MODIS Land Cover (MCD12Q1 and MCD12C1) Products. https://wwwgooglecom/url?sa=t&rct=j&q=&esrc=s&source=web&cd=&cad=rja&uact=8&ved=2ahUKEwjAu7ag-prrAhXJXhUIHcdwBIsQFjAAegQIBhAB&url=https%3A%2F%2Flpdaacusgsgov%2Fdocuments%2F101%2FMCD12_User_Guide_V6pdf&usg=AOvVaw2DOz6CWt3DliUmRcor6YV1.
Sulla-Menashe, D., Gray, J.M., Abercrombie, S.P., Friedl, M.A., 2019. Hierarchical mapping of annual global land cover 2001 to present: the MODIS Collection 6 Land Cover product. Rem. Sens. Environ. 222, 183–194.
Sun, Ge, Zuo, C., Liu, S., Liu, M., McNult, S.G., Vose, J.M., 2008. Watershed evapotranspiration increased due to changes in vegetation composition and structure under a subtropical climate. J. Am. Water Resour. Assoc. 44 (5), 1164–1175.
Takata, K., Hanasaki, N., 2020. The effects of afforestation as an adaptation option: a case study in the upper Chao Phraya River basin. Environ. Res. Lett. 15, 044020.
Teuling, A.J., de Badts, E.A.G., Jansen, F.A., Fuchs, R., Buitink, J., van Dijke, A.J.H., Sterling, S.M., 2019. Climate change, reforestation/afforestation, and urbanization impacts on evapotranspiration and streamflow in europe. Hydrol. Earth Syst. Sci. 23, 3631–3652.
Thiha, S., Shamseldin, A.Y., Melville, B.W., 2020. Assessment of the Myitnge River flow responses in Myanmar under changes in land use and climate. Model Earth Syst. Environ.
Wangpimool, W., Pongput, K., Sukvibool, C., Sombatpanit, S., Gassman, P.W., 2013. The effect of reforestation on stream flow in Upper Nan river basin using soil and water assessment tool (SWAT) model. Int. Soil Water Conserv. Res. 1, 53–63.
Warburton, M.L., Schulze, R.E., Jewitt, G.P.W., 2012. Hydrological impacts of land use change in three diverse South African catchments. J. Hydrol. 414–415, 118–135.
Wen, X., Lu, S., Jin, J., 2012. Integrating remote sensing data with WRF for improved simulations of oasis effects on local weather processes over an arid region in northwestern China. J. Hydrometeorol. 15, 573–587.
Yin, D., Xue, Z.G., Gochis, D.J., Yu, W., Morales, M., Rafieeinasab, A., 2020. A process-based, fully distributed soil erosion and sediment transport model for WRF-hydro. Water 12, 1840.
Yira, Y., Diekkrüger, B., Steup, G., Bossa, A.Y., 2016. Modeling land use change impacts on water resources in a tropical West African catchment. J. Hydrol. 537, 187–199.
Yucel, I., Onen, A., Yilmaz, K.K., Gochis, D.J., 2015. Calibration and evaluation of a flood forecasting system; utility of numerical weather prediction model, data assimilation and satellite-based rainfall. J. Hydrol. 523, 49–66.
Zhang, C., Wang, Y., Hamilton, K., 2011. Improved representation of boundary layer clouds over the Southeast Pacific in ARW-WRF using a modified tiedtke cumulus parameterization scheme. Mon. Weather Rev. 139, 3489–3513.
Zhang, M., Liu, N., Harper, R., Li, Q., Liu, K., Wei, X., Ning, D., Hou, Y., Liu, S., 2017. A global review on hydrological responses to forest change across multiple spatial scales: importance of scale, climate, forest type and hydrological regime. J. Hydrol. 546, 44–59.
Zheng, H., Chen, F., Ouyang, Z., Tu, N., Xu, Weihua, Wang, X., Miao, H., Li, X., Tian, Y., 2008. Impacts of reforestation approaches on run-off control in the hilly red soil region of southern China. J. Hydrol. 356, 174–184.
Zhou, Y., 2014. Watershed Hydrology and Land-Use and Land-Cover Change (LULCC) in Book: Encyclopedia of Natural Resources: Water Publisher. Taylor & Francis, Project.
Zhou, Y., Wang, Y.Q., 2008. Extraction of impervious surface areas from high spatial resolution imagery by multiple agent segmentation and classification. Photogramm. Eng. Rem. Sens. 74 (7), 857–868.